TITLE PAGE

Classification:

PHYSICAL SCIENCES: Sustainability Science

BIOLOGICAL SCIENCES: Environmental Sciences

Title:

Robust paths to net greenhouse gas mitigation and negative emissions *via* advanced biofuels

Authors:

John L. Field[a,†], Tom L. Richard[b], Erica A. H. Smithwick[c], Hao Cai[d], Mark S. Laser[e], David S. LeBauer[f], Stephen P. Long[g,h], Keith Paustian[a,i], Zhangcai Qin[d,j,k], John J. Sheehan[l,m], Pete Smith[n], Michael Q. L. Wang[d], Lee R. Lynd[e,†]

Authors Affiliations:

[a]Natural Resource Ecology Laboratory, Colorado State University, Fort Collins, CO 80523

[b]Department of Agricultural and Biological Engineering, The Pennsylvania State University, University Park, PA 16802

[c]Department of Geography and Earth and Environmental Systems Institute, The Pennsylvania State University, University Park, PA 16802

[d]Energy Systems Division, Argonne National Laboratory, Lemont, IL 60439

[e]Thayer School of Engineering, Dartmouth College, Hanover, NH 03755

[f]Arizona Experiment Station, University of Arizona, Tucson, AZ 85721

[g]Department of Crop Sciences, University of Illinois at Urbana-Champaign, Urbana, IL, 61801
[h]Lancaster Environment Centre, Lancaster University, Lancaster, LA1 4YQ UK
[i]Department of Soil and Crop Sciences, Colorado State University, Fort Collins, CO 80523
[j]School of Atmospheric Sciences and Guangdong Province Key Laboratory for Climate Change and Natural Disaster Studies, Sun Yat-sen University, Zhuhai, Guangdong 510245, China
[k]Southern Marine Science and Engineering Guangdong Laboratory, Zhuhai 519082, China
[l]School of Agricultural Engineering (FEAGRI), University of Campinas, Campinas, SP, 13083-875, Brazil
[m]Department of Chemical and Biological Engineering, Colorado State University, Fort Collins, CO 80523
[n]Institute of Biological and Environmental Sciences, University of Aberdeen, Aberdeen AB24 3UU, UK
[†]These authors contributed equally to this work

Corresponding Author:
John L Field
Natural Resource Ecology Laboratory, 1499 Campus Delivery, Colorado State University, Fort Collins, Colorado, 80523-1499, USA
(317) 748-9792
<John.L.Field@gmail.com>

Keywords:

Biofuels; BECCS; natural climate solutions; mitigation; negative emissions; ecosystem modeling; life cycle assessment

ABSTRACT

Biofuel and bioenergy systems are integral to most climate stabilization scenarios for displacement of transport sector fossil fuel use, and for producing negative emissions *via* carbon capture and storage (CCS). However, the net greenhouse gas mitigation benefit of such pathways is controversial due to concerns around ecosystem carbon losses from land use change, and foregone sequestration benefits from alternative land uses. Here we couple bottom-up ecosystem simulation with models of cellulosic biofuel production and CCS in order to track ecosystem and supply chain carbon flows for current and future biofuel systems, in comparison to competing land-based biological mitigation schemes. Analyzing three contrasting U.S. case study sites, we show that on land transitioning out of crops or pasture, switchgrass cultivation for cellulosic ethanol production has per-hectare mitigation potential comparable to reforestation and several-fold greater than grassland restoration. In contrast, harvesting and converting existing secondary forest at those sites incurs large initial carbon debt requiring long payback periods. We also highlight how plausible future improvements in energy crop yields and biorefining technology together with CCS would achieve mitigation potential 4 and 15 times greater than forest and grassland restoration, respectively. Finally, we show that recent estimates of induced land use change are small relative to the opportunities for improving system performance that we quantify here. While climate and other ecosystem service benefits cannot be taken for granted from cellulosic biofuel deployment, our scenarios illustrate how conventional and carbon-negative biofuel systems could make a near-term, robust, and distinctive contribution to the climate challenge.

SIGNIFICANCE STATEMENT

The climate benefits of cellulosic biofuels have been challenged based on carbon debt, opportunity costs, and indirect land use change, prompting calls for withdrawal of R&D support. Using a quantitative ecosystem modelling approach which differentiates primary production, ecosystem carbon balance, and biomass harvest more explicitly than previous assessments, we show that none of these arguments preclude cellulosic biofuels from realizing greenhouse gas mitigation. Our assessment illustrates how deliberate land use choices support the climate performance of current-day cellulosic ethanol technology, and how technological advancements and carbon capture and storage addition could produce several times the climate mitigation potential of competing land-based biological mitigation schemes. These results affirm the climate mitigation logic of biofuels, consistent with their prominent role in many climate stabilization scenarios.

TEXT

Climate stabilization plans—particularly those that aim to limit warming below 1.5 °C—rely on land-based biological mitigation (1) from bioenergy production and terrestrial carbon sequestration as a unique and essential complement to renewable energy deployment and other greenhouse gas (GHG) mitigation measures across all emissions sectors (2, 3). Liquid biofuel production is currently among the most technologically mature and cost-effective routes to decarbonizing aviation, shipping, long haul transport, and residual non-electrified light-duty transport (4, 5). In addition, bioenergy systems can contribute to large-scale carbon dioxide removal (CDR) *via* carbon sequestration in soils on which feedstock crops are cultivated (depending on former land use) (6) and *via* bioenergy with carbon capture and storage (BECCS) (7) or biochar co-production (8). While much BECCS planning to date has focused on electricity-producing systems, the high-purity byproduct CO_2 streams from biofuel production do not require separation and concentration steps, and thus are an efficient and low-cost target for near-term CCS deployment (9). Achieving significant bioenergy-based GHG mitigation at useful timescales implies a scale-up of biomass feedstock cultivation and a build-out of associated logistics, conversion, and perhaps CCS infrastructure at rapid rates (10, 11).

The underlying logic of GHG mitigation through biofuels and bioenergy production has, however, been repeatedly challenged. While material and energy inputs into biofuel production supply chains are well-studied (12), more recent critiques focus on whether feedstock crops can be sustainably sourced without self-defeating reductions in ecosystem carbon storage. Conversion of non-agricultural land with high initial carbon stocks to the cultivation of corn or other first-generation biofuel feedstock crops can result in large up-front ecosystem carbon storage reductions ('carbon debt') that must be overcome *via* subsequent fossil fuel displacement or carbon sequestration before net mitigation is achieved (13). Conversion of existing productive agricultural land with low carbon stocks can also be counterproductive if the loss of commodity production there leads to compensatory agricultural expansion (and associated ecosystem carbon losses) elsewhere, an effect known as indirect land use change or 'ILUC' (14). ILUC concerns may be minimized or avoided by targeting feedstock production on low-productivity, environmentally sensitive, or abandoned cropland (15, 16), or on land 'spared' from continued agricultural use through future agricultural intensification or dietary shifts (17, 18). However, since reforestation offers an alternative use of such land for biological mitigation, it has been suggested that bioenergy assessments should consider the 'opportunity cost' of the foregone ecosystem carbon sequestration of reforestation when land is used instead for feedstock production (19).

While each of these ideas was originally applied to first-generation biofuels from food crops, critiques around carbon debt (20), ILUC (21), and opportunity costs (22, 23) have all subsequently been invoked for the production of cellulosic biomass to use in electricity generation or advanced biofuel production. Synthesizing these and other sustainability concerns, recent studies have suggested that the dedicated use of land for biomass feedstock production results in sub-optimal climate outcomes (24), and have recommended re-focusing research efforts and policy support away from bioenergy technology, towards land-based biological carbon management (25). However, those conclusions are often based on secondary estimates of bioenergy system performance and mitigation opportunity costs, and generally exclude consideration of CCS or future technology improvements. Researchers have also called for more biophysically-explicit assessments that establish bioenergy system mitigation in terms of increased net carbon fluxes from the atmosphere into feedstock-producing ecosystems (*via* either increased carbon fixation or reduced respiration, so-called ‘additional carbon’) (26–29).

Here we couple ecological, engineering, and life cycle emissions accounting models to estimate the biophysical potential of perennial energy grass cultivation and biofuel production to replace fossil energy sources and/or directly sequester carbon, in comparison to other land-based biological mitigation schemes. A process-based ecosystem model was calibrated to perform temporally-explicit simulation of atmosphere–biosphere carbon exchanges under different land use choices at three case study sites, modeling both current and projected future energy grass productivity. We conducted a factorial analysis estimating the net biophysical GHG mitigation potential of cellulosic biofuel production considering different initial land uses (cropland, pasture, and secondary forest), energy grass yields (current and anticipated future), and biorefinery technology configurations (current biochemical conversion to ethanol, future hybrid conversion to ethanol and Fischer-Tropsch liquids, and future conversion with CCS), accounting for upstream life cycle production inputs. We compare those net biofuel mitigation potential results to that of reforestation or grassland restoration on former agricultural land or continued undisturbed growth of secondary (70-year-old aggrading) forest. The analysis shows that many, but not all, of the cellulosic biofuel production scenarios considered achieve greater GHG mitigation potential than alternate land uses. This case study-based assessment quantifies the biophysical mitigation potential of biofuel production systems as affected by initial land use and biorefining technology. Biofuel production economics, sustainable deployment scale, and impacts on biodiversity and other ecosystem services fall outside the scope of this analysis. We show that several bioenergy system design factors that we analyzed (initial land cover, feedstock production and conversion technology, and CCS) have substantially larger impact on system mitigation performance than previous estimates of indirect land use change from growing cellulosic crops.

Ecosystem productivity & carbon storage

Terrestrial ecosystem carbon accounting requires careful differentiation between the gross rate of plant photosynthesis (gross primary production or GPP), the net rate of biomass carbon accumulation accounting for autotrophic respiration (net primary production or NPP), ecosystem carbon storage accounting for heterotrophic respiration (R_h) in soils and fauna (net ecosystem production or NEP), and the change in total ecosystem carbon storage accounting for biotic and abiotic disturbance events, lateral losses, and harvests (net ecosystem carbon balance or NECB) (30). Land use change for bioenergy production or other mitigation purposes results in changes to NECB that reflect previous land use; the productivity, structure, and longevity of the subsequent vegetation; and carbon removal from periodic biomass harvest or other disturbance. However, while comprehensive measurement of these ecosystem carbon fluxes can be conducted in energy crop field experiments (31, 32), such accounting is rarely invoked in model-based bioenergy sustainability assessments (22). Process-based ecosystem models provide a framework for synthesizing discrete measurements of carbon stocks and fluxes over time, with mechanistic representations of ecosystem function to facilitate wider extrapolation and scenario evaluation. The DayCent model utilized here features daily calculation of NPP and carbon re-distribution and respiration losses from biomass, litter, and soil carbon pools as affected by local climate, soil (edaphic) factors; vegetation productivity, structure, and phenology; and management (e.g., tillage, fertilizer application) practices (33).

Our analysis considered three contrasting case study sites in the U.S. east of the 100th meridian covering a range of climates (Fig. S1) and ecosystem types, including two sites (Webster County, Iowa, and La Salle Parish, Louisiana) near the forest–grassland transition zone at the margin of the Great Plains region, and an additional site (Wayne County, New York) in the eastern U.S. where forest is the more common natural land cover. We used DayCent to conduct 70-year forward simulations of productivity and changes in ecosystem carbon storage and soil nitrous oxide (N_2O) emissions at these sites for the conversion of cropland, pasture, and secondary forest to managed perennial energy grass (switchgrass, *Panicum virgatum*) or a natural vegetation alternative (reforestation, grassland restoration, or continued secondary forest growth; Fig. S2). We calibrated DayCent to best match carbon and nitrogen cycling observed in U.S. switchgrass (*Panicum virgatum*) field trials (34) and for regionally-specific secondary forest growth (35). Anticipating ongoing productivity improvements through breeding, we also modeled a ‘future’ switchgrass variety that achieves 64% higher yield, equivalent to a 2% annual improvement compounded over 25 years. For comparison, the U.S. Department of Energy’s 2016 Billion Ton Report considers annual yield increase scenarios of 1, 2, 3, and 4% (36).

Figure 1 shows ecosystem carbon cycling for the different scenarios averaged annually over the first 30 years of simulation in DayCent, a time period selected for near-term policy relevance and consistency with previous analysis (37). Simulated NPP is substantially higher for managed switchgrass cultivation (7–19 Mg C ha^{-1} y^{-1}) than for unmanaged reforestation or grassland restoration (2–7 Mg C ha^{-1} y^{-1}) on former cropland and pasture due to the higher yield potential of improved switchgrass varieties and reduced nutrient limitations after fertilizer addition (Fig. 1 and Table S1). Our yield estimates for managed current-day switchgrass (10–14 Mg biomass ha^{-1} y^{-1}) compare well with other estimates, whereas our future switchgrass yields (16–22 Mg biomass ha^{-1} y^{-1}) are similar to current-day Miscanthus yields in the Midwest (38).

Our NECB estimates ranged from 0.1 to 1.1 Mg C ha^{-1} y^{-1} increases in soil C stocks for managed switchgrass. Agricultural land reforestation scenarios achieved much higher NECB (1.0–3.4 Mg C ha^{-1} y^{-1}, corresponding on average to 61% of annual NPP), mostly through accumulation of aboveground woody biomass. Grassland restoration, in which herbaceous aboveground biomass senesces each season and only a fraction of the carbon therein is ultimately retained as litter or soil organic matter, had NECB comparable to the managed switchgrass scenarios (0.5–1.0 Mg C ha^{-1} y^{-1}, equivalent to 15% of NPP in those systems). In contrast, harvest of existing secondary forest and replacement with switchgrass resulted in significant net reductions in ecosystem carbon storage that persisted after 30 years (equivalent to an annualized loss rate of 3.6–7.2 Mg C ha^{-1} y^{-1}). These scenarios include carbon export from the system *via* both tree biomass removal during land conversion (Harv– wood) and annual harvest of the switchgrass subsequently cultivated at the site (Harv– switchgrass); the ultimate fate of that removed biomass carbon is detailed in subsequent sections. Cumulative above- and below-ground NECB for all scenarios over the full course of the 70-year DayCent simulations are shown in Fig. S3. Aboveground carbon accumulates steadily in the reforestation and continued secondary forest growth scenarios, but is negligible in the grassland and switchgrass scenarios. Most scenarios show increases in belowground carbon storage, though in many cases this sequestration attenuates over the course of the 70-year simulation as soil carbon reaches a new equilibrium value.

In the switchgrass scenarios, on average 67% of seasonal NPP is harvested as biomass. Comparing across scenarios, current-day switchgrass cultivation achieves only 14% of the ecosystem carbon sequestration of reforestation ($NECB_{bfuel}$:$NECB_{veg,forest}$). However, for every Mg of reforestation carbon sequestration that is foregone in the biofuel scenario, 2.5 Mg of carbon is harvested as biomass ($Harv_{bfuel}$:$NECB_{veg,forest}$). Future higher-yielding switchgrass varieties would sequester 28% as much as reforestation, and yield 4.0 Mg biomass-C for every tonne of foregone reforestation carbon sequestration. Respiration losses represent a fundamental limitation on the ability of ecosystems to accumulate carbon (39), and the harvest of senesced herbaceous biomass removes carbon from the ecosystem that would otherwise largely be respired. This feedstock thus meets previously proposed system additionality requirements (25, 28).

Conversion technology & carbon flows

Our analysis considered future improvements in biofuel conversion technology in addition to the increases in switchgrass yield described previously. Our ‘current’ cellulosic biofuel technology case consisted of dilute acid pretreatment followed by simultaneous saccharification and fermentation to ethanol (40), similar to that deployed in existing commercial-scale cellulosic biorefineries. The ‘future’ biofuel case considered ammonia fiber expansion pretreatment and consolidated bioprocessing to ethanol, followed by gasification and Fischer-Tropsch (FT) upgrading of fermentation residues (40, 41). In both cases the remaining conversion by-products are combusted to meet biorefinery steam and power requirements, with any excess electric power exported to the grid. We also considered a BECCS variant of the future biofuel case in which the high-purity CO_2 streams from fermentation, syngas cleanup, and power island fuel gas cleanup (which together account for half of all feedstock carbon entering the biorefinery; Table S1) were de-watered, compressed, and injected into geological storage, rather than vented to the atmosphere.

We compared the biophysical GHG mitigation potential of these biofuel and BECCS scenarios (together abbreviated as ‘bfuel’) to that of alternative scenarios of natural vegetation restoration or retention (‘veg’). System boundaries and relevant flows of carbon between the atmosphere, biosphere, and geosphere are illustrated in Fig. 2. Cumulative ecosystem carbon sequestration or loss from our case study sites is described in terms of NPP, R_h, Harv, and NECB as detailed previously. The carbon in this harvested biomass is ultimately returned to the atmosphere when emitted from the biorefinery during biofuel production (BP, which includes CO_2 emissions from both fermentation and the combustion of non-fermented residues), or when emitted from a vehicle tailpipe during biofuel use (TP_{bfuel}). Biofuel production incurs additional biofuel supply chain (BSC) emissions (e.g., farm inputs and energy use, biomass transport, etc.), but avoids tailpipe emissions of fossil carbon (TP_{veg}) and gasoline supply chain (GSC) emissions (e.g., petroleum extraction, refining, and distribution) present in the vegetation restoration scenarios. In BECCS scenarios, biorefinery BP emissions are instead captured and put into geologic storage (CCS). In scenarios of secondary forest conversion to switchgrass we assumed that all initial aboveground forest biomass would be harvested and used as a bioenergy feedstock; we did not consider co-production of timber and other durable wood products, or land clearing via wasteful biomass burning. Indirect effects (e.g., ILUC) are not included in the direct emissions accounting described here, but are explored subsequently.

Land-based biological mitigation scenario performance

We estimated the net biophysical GHG mitigation potential of each analysis scenario by converting the simulated ecosystem carbon storage changes shown in Fig. 1 to carbon dioxide equivalent values, and adding fossil fuel displacement effects, upstream supply chain life cycle impacts (agricultural inputs and farm operations, fossil fuel extraction and refining, etc.), and geological carbon sequestration *via* CCS (see Methods for details). Figure 3 illustrates the cumulative direct GHG mitigation potential of the biofuel/BECCS and the natural vegetation restoration/retention scenarios over time. Mitigation is realized immediately for the conversion of former agricultural land to natural vegetation or to biofuel production, due to increases in ecosystem carbon storage and displacement of conventional gasoline with biofuels, respectively. In contrast, secondary forest conversion to biofuel production (using both the harvested wood and subsequently cultivated switchgrass as feedstocks) incurs a large initial carbon deficit which is not repaid by biofuel production with current technology over the 70-year simulation period. Future biofuel technology requires 27–52 years to achieve parity with the ‘continued growth’ forest baseline (i.e., to make up the opportunity cost of devoting that land to switchgrass production), though the addition of CCS reduces this payback period down to 6–8 years.

Figure 4A details the average annual mitigation potential of each scenario over the first 30 years of simulation. The mitigation potential of reforestation (3.4–11.9 Mg CO_2e ha^{-1} y^{-1}) and grassland restoration (1.7–3.5 Mg CO_2e ha^{-1} y^{-1}) on former agricultural land reflects changes in NECB and ecosystem N_2O emissions, with inter-site variability driven by climate, soils, plant phenology, and initial soil carbon stocks. Switchgrass cultivation on former agricultural land sequesters soil carbon at a rate of 0.5–3.3 Mg CO_2e ha^{-1} y^{-1}. Biofuel production also incurs benefits from avoided fossil fuel emissions (AFFE, defined as the sum of TP_{veg} and GSC). AFFE averages 7.4 and 19.9 Mg CO_2e ha^{-1} y^{-1} for the current and future cellulosic biofuel production scenarios, respectively. This gross GHG displacement is reduced 11–35% by biofuel supply chain and soil N_2O emissions. However, current cellulosic biofuel technology still achieves a mean net mitigation potential of 6.0 Mg CO_2e ha^{-1} y^{-1} across all three sites and previous agricultural land uses (excluding the secondary forest conversion scenarios), which is within the range of previous model-based analyses (42). This mitigation value falls within our estimated range for reforestation on former agricultural land, and is 250% greater than that of grassland restoration. In contrast, clearing secondary forest for switchgrass production results in a large up-front loss of ecosystem carbon storage (i.e., negative NECB) that is not offset by fossil fuel displacement via current-day cellulosic ethanol production (using both the harvested wood and subsequently-cultivated switchgrass) over the first 30 years of the assessment.

Future BECCS systems offer improved performance through higher switchgrass and fuel yields and the direct geological sequestration of CO_2 in amounts greater than the reforestation carbon sink (Table S1). Comparative carbon fluxes for the reforestation and future BECCS scenarios on abandoned cropland are illustrated in Figs. 4B and 4C, respectively. Fig. S4 presents mitigation results normalized by NPP for bioenergy and vegetation restoration on abandoned cropland, to illustrate whether higher-performing scenarios are more effective at achieving mitigation per unit of carbon fixed, or simply fix more carbon per hectare. Reforestation achieves 0.6 metric tonnes of net ecosystem carbon storage for every Mg of net primary production carbon (Mg NPP-C). The future BECCS scenario achieves a comparable NPP-normalized net mitigation potential of 0.7 Mg C-equivalent per Mg NPP-C via a combination of ecosystem carbon storage, net fossil fuel displacement, and CCS. However, total NPP for future switchgrass production is on average approximately three-and-a-half times higher than that of unmanaged secondary forest regrowth. Together, this results in four times the total per-hectare net mitigation potential for the future BECCS scenario as compared to reforestation. Similarly, the NPP-normalized net mitigation potential of current-day switchgrass ethanol (0.2 Mg Ce (Mg NPP-C)$^{-1}$) is only about 20% higher than that of grassland restoration, but managed switchgrass production achieves approximately twice the NPP, resulting in 2.5 times more total mitigation than grassland restoration. Most starkly, the future BECCS scenario achieves approximately five times the NPP-normalized net mitigation and three times the total NPP of grassland restoration, which combined result in ~15x the total mitigation potential compared to that scenario.

Indirect emissions in perspective

The analysis presented thus far has accounted for the direct GHG impacts of cellulosic biofuel production or natural vegetation restoration/retention as illustrated in Fig. 2. These estimates likely capture the full GHG impact of those scenarios when deployed on retired or abandoned cropland (15) or in cases of 'land-sparing' *via* future agricultural intensification (17) or dietary shifts (18). Wider-scale deployment of biofuel and other land-based CDR technologies in competition with existing agriculture incurs risk of ILUC effects (14). External estimates of such ILUC emissions can theoretically be added to the direct GHG impacts assessed here to estimate total net life cycle GHG impacts (43) in those cases. However, most recent economic assessment studies report only total ***induced*** land use change (LUC), a metric that aggregates together both ILUC and the 'direct' changes in carbon storage in the fields where biofuel feedstock crops are grown (Fig. S5). Sometimes this total induced LUC is broken down into domestic and international components. In practice it is often impossible to harmonize and down-scale such estimates (which reflect economically optimal land use responses at very coarse spatial scales) to the more targeted land conversion scenarios of our assessment. It is nonetheless still illustrative to compare the magnitude of these prior literature estimates to the bioenergy system design factors assessed here.

Figure 5 shows our modeling results alongside estimates of total induced LUC emissions for cellulosic biofuel production from perennial grasses (switchgrass, Miscanthus, or unspecified) compiled from various prior analyses (44) and from the Argonne National Laboratory CCLUB model (45), as summarized in Table S2. The average biomass yield assumed across the studies that considered a switchgrass feedstock (13.1 Mg ha^{-1} y^{-1}) is within the range simulated for our present-day switchgrass biofuel scenarios. The average yield assumed across the studies that considered a Miscanthus feedstock (17.5 Mg ha^{-1} y^{-1}) is representative of current yields for that crop, and consistent with our higher-yielding future switchgrass biofuel scenarios (see Methods– DayCent modeling). These studies considered cellulosic ethanol production at scales of 27–34 billion gallons of ethanol annually, approximately half the amount of cellulosic biofuel mandated by the US Energy Independence and Security Act of 2007 (46). This scale is smaller than that called for in some climate stabilization scenarios (7), and such wider bioenergy deployment could lead to larger indirect emissions consequences.

Total induced LUC estimates range from a net emission of 3.3 Mg CO_2e ha^{-1} y^{-1} to a net sequestration of 1.9 Mg CO_2e ha^{-1} y^{-1}. The average for the switchgrass studies is a net emission of 1.13 Mg CO_2e ha^{-1} y^{-1}, and the average across all studies is a net emission of 0.13 Mg CO_2e ha^{-1} y^{-1}. While the highest total induced LUC estimates are of comparable magnitude to our estimates of the direct mitigation potential from grassland restoration, they are significantly smaller than our estimates of the direct mitigation potential from current-day cellulosic ethanol production. Our analysis suggests that cellulosic biofuel system GHG performance can be improved by 14 Mg CO_2e ha^{-1} y^{-1} by cultivating switchgrass feedstock on former pasture rather than converting secondary forest, or by an additional 3 Mg CO_2e ha^{-1} y^{-1} by targeting cropland over pasture. Future switchgrass and biofuel yield improvement and CCS adoption can improve the biophysical mitigation potential of biofuel systems by a further 15 and 17 Mg CO_2e ha^{-1} y^{-1}, respectively. The international share of total induced LUC estimates are broken out where possible in Table S2. Our average estimates for the mitigation potential of current-day biofuel and future BECCS scenarios, respectively, are 12 and 68 times greater than the average of all international land use change emissions estimates, and 3 and 18 times greater than the highest estimate.

There are other potential indirect effects of biofuel deployment beyond ILUC. Geographically uneven adoption of GHG mitigation policies could cause biofuel use in one country to lower global petroleum prices, leading to higher petroleum consumption elsewhere (i.e., a rebound effect). The magnitude and even sign of such an emissions effect from the deployment of first-generation food-based biofuels are disputed (47, 48), and depend heavily on the exact structure of biofuel support and the presence of other GHG mitigation policies (e.g., carbon taxes or emissions trading schemes) both domestically and globally. A large rebound effect could potentially offset much of the AFFE value of the conventional cellulosic biofuel systems assessed here (Fig. 4A). Rebound has only received a small fraction of the research attention that ILUC has and deserves further study, particularly since the question of whether renewable energy sources displace or supplement fossil fuel usage is not limited to biofuels (49). However, even in the absence of fossil fuel displacement benefits, we assess that future carbon-negative biofuel–CCS systems could still out-perform reforestation based on their geological sequestration value alone (an effect not subject to such indirect market-based risks).

Discussion

Bioenergy assessment and policy development have often been limited by the simplifying but inaccurate assumption of biomass carbon neutrality (50, 51). In response, a variety of studies (26–28) have called for explicit accounting of ecosystem carbon fluxes as an alternative to the carbon neutrality assumption, and for comparison to alternative land uses in order to better understand the true biophysical mitigation potential of bioenergy systems (19, 22, 23, 42, 52). Our analysis addresses both points, using well-calibrated models of ecosystem carbon fluxes and stocks to evaluate both bioenergy and alternate land use scenarios. We find that:

- Biofuel production from switchgrass cultivated on former agricultural lands avoids *carbon debt*, resulting in immediate net mitigation potential (Fig. 3). Conversion of secondary forest to biofuel production results in ecosystem carbon debts requiring several years to several decades or more to overcome, depending on conversion technology and whether CCS is employed.

- Current-day cellulosic biofuel production on former agricultural land results in much greater mitigation potential than that of grassland restoration, and similar to the carbon *opportunity cost* of reforestation at sites that would support forest (Figs. 3 & 4). Future technology improvement and CCS integration could further improve bioenergy system per-hectare mitigation potential by a factor of approximately six relative to current-day performance.
- Several factors analyzed in this study—initial land cover, maturity of production technology, and CCS use—have much larger impacts on mitigation performance than recent literature estimates of both total induced land use change and international land use change effects associated with perennial grass feedstock cultivation (Fig. 5).

There is growing recognition that implementation of land-based biological mitigation strategies needs to be both rapid and robust. In this context, it should be noted that biomass production for bioenergy generates new revenue streams for landowners outside of payment schemes for carbon or other ecosystem services, which could help incentivize quicker or more widespread adoption of land-based biological mitigation. In addition, bioenergy systems configured for negative emissions *via* CCS (as assessed here) or biochar co-production (8) are likely to achieve durable geological and soil carbon sequestration with less vulnerability to future changes in land use, disturbance regimes (e.g., wildfire, insect outbreaks), or local climate shifts that could reduce the mitigation value of restored grasslands or especially forests (53, 54). Our mitigation estimates for vegetation restoration are generous in that we did not explicitly simulate potential disturbance (focusing on NECB instead of the more widely-scoped net biome production metric (30)) or consider how periodic harvest could be managed spatially to maintain consistent carbon storage at landscape scales (55).

There are many other considerations in land management besides GHG mitigation, and landowners often have to navigate trade-offs between creating economic value and maintaining or enhancing biodiversity and ecosystem services (56). The rapid scale-up of any land-based mitigation or CDR scheme will challenge assessment practice and governance structures to ensure sustainable and desirable outcomes (57). However, greater consideration of land management for climate change mitigation will almost certainly be necessary to achieve climate stabilization goals, with or without bioenergy (2, 3). That is likely best achieved through development of a portfolio of multiple land-based biological mitigation options (1), and the most useful corresponding assessments are those which can support decision-making and optimization among the competing options in different locations and contexts. In addition to the biophysical potential for GHG mitigation as assessed here, decision criteria should include factors outside the scope of this analysis such as costs, wildlife and biodiversity impacts, other ecosystem services, and sustainable development and social equity outcomes as compared to status-quo land use and other land-based mitigation alternatives.

Our results—particularly those for future biofuel technology scenarios—stand in sharp contrast to recent critiques that advocate eliminating policy support for bioenergy research (25) and deployment (24). We note that continued research, development, and iterative limited-scale deployment of such systems is essential for realizing improvements and cost reductions in biorefining and CCS technology (58, 59) in support of existing renewable fuel mandates and in time for the mid-century wide-scale deployment of CDR called for in many projections. Furthermore, real-world empirical data on energy crop adoption and performance (37, 60) informs assessment science and provides guidance for ongoing bioenergy policy development. Net GHG mitigation is not an automatic outcome of any bioenergy system, and previous studies have illustrated a number of sustainability pitfalls that can erode system GHG benefits. However, these pitfalls are avoidable if the bioenergy industry and policymakers are mindful of them and design bioenergy systems and corresponding land use policies with intent accordingly. In particular, we show that cellulosic biofuels can be deployed today without significant carbon debt, and achieve greater mitigation potential than restoration of natural vegetation in the case of grasslands. Moreover, the mitigation potential of projected future biofuel technology is several-fold higher. Across a wide range of land use and natural vegetation types, sustainable bioenergy systems can make an important and distinctive contribution to the climate stabilization challenge.

Materials and Methods

Carbon & mitigation accounting

Net ecosystem carbon balance (NECB) (30, 61) can be expressed in terms of changes in above- and belowground carbon stocks (ΔC_{AG} and ΔC_{BG}, respectively), or alternately in terms of the fluxes net primary production (NPP), heterotrophic respiration (R_h), and carbon in harvested biomass (Harv) as follows (detailed derivation available in the Supplementary Information):

$$NECB = \Delta C_{AG} + \Delta C_{BG} = NPP - R_h - Harv \qquad [1]$$

The net cumulative direct carbon-equivalent GHG exchange with the atmosphere (ΔC_{atm}) associated with a marginal increase in biofuel production (‘bfuel’) as illustrated in Fig. 2 over a given assessment period is:

$$\Delta C_{atm,bfuel} = BSC + BP + TP_{bfuel} + R_{h,bfuel} - NPP_{bfuel} \qquad [2]$$

which includes biofuel supply chain (BSC) life cycle emissions associated with material inputs and energy use during switchgrass cultivation, harvest, and transport, as well as soil N_2O emissions; biorefinery emissions of the biogenic CO_2 by-product of biofuel production (BP); tailpipe emissions of biogenic carbon from biofuel combustion (TP_{bfuel}), and ecosystem carbon exchanges with the atmosphere, specifically net primary production (NPP_{bfuel}) and heterotrophic respiration ($R_{h,bfuel}$). Combining equations [1] and [2], this net atmospheric exchange can alternately be expressed in terms of changes in above- and below-ground ecosystem carbon storage ($\Delta C_{AG,bfuel}$ and $\Delta C_{BG,bfuel}$, respectively) and biomass harvest:

$$\Delta C_{atm,bfuel} = BSC + BP + TP_{bfuel} - \left(\Delta C_{AG,bfuel} + \Delta C_{BG,bfuel}\right) - Harv \quad [3]$$

Assuming negligible supply chain biomass losses, a biorefinery carbon balance implies that a fraction of harvested biomass carbon will be converted to biofuel and re-emitted from vehicle tailpipes, and the remainder will be either emitted at the biorefinery (BP) or geologically sequestered via carbon capture and storage (CCS):

$$Harv = BP + CCS + TP_{bfuel} \quad [4]$$

Combining equations [3] and [4], the effect of the biofuel scenario on the atmosphere can be expressed more simply as new biofuel supply chain emissions minus net ecosystem sequestration and geological carbon sequestration:

$$\Delta C_{atm,bfuel} = BSC - \left(\Delta C_{AG,bfuel} + \Delta C_{BG,bfuel}\right) - CCS \quad [5]$$

The net cumulative direct exchange with the atmosphere in an alternative natural vegetation restoration scenario (‘veg’) can be expressed similarly. However, the ‘veg’ scenarios lack biomass harvest but include baseline conventional gasoline supply chain and tailpipe emissions (GSC and TP_{veg}, respectively) in energy-equivalent amounts equal to biofuel production in the biofuel scenario (assuming that biofuel production offsets gasoline use on a 1:1 energy basis, ignoring any rebound effect):

$$\Delta C_{atm,veg} = GSC + TP_{veg} - \left(\Delta C_{AG,veg} + \Delta C_{BG,veg}\right) \quad [6]$$

Land-based biological mitigation is the purposeful management of land and photosynthetically-derived carbon to reduce the net accumulation of CO_2 and other GHGs in the atmosphere resulting from fossil fuel usage and biosphere losses, *via* the displacement of fossil energy emissions and/or the direct sequestration of carbon. We thus calculate the net biophysical mitigation (NM) potential of a scenario as the opposite of the net cumulative direct carbon exchange with the atmosphere, minus fluxes associated with baseline fossil fuel usage (GSC and TP_{veg}). For the ‘veg’ scenarios, we build on equation [6] to calculate:

$$NM_{veg} = -\left(\Delta C_{atm,veg} - \left(GSC + TP_{veg}\right)\right)$$

$$= -\left(\left(GSC + TP_{veg} - \left(\Delta C_{AG,veg} + \Delta C_{BG,veg}\right)\right) - \left(GSC + TP_{veg}\right)\right)$$

$$= \Delta C_{AG,veg} + \Delta C_{BG,veg} \quad [7]$$

Since there is no displacement of conventional gasoline use in this scenario, land-based biological mitigation consists only of the net cumulative amount of carbon sequestered in above- and below-ground ecosystem carbon pools over the assessment period. The equivalent for the biofuel scenarios is:

$$NM_{bfuel} = -\left(\Delta C_{atm,bfuel} - \left(GSC + TP_{veg}\right)\right)$$

$$= -\left(\left(BSC - \left(\Delta C_{AG,bfuel} + \Delta C_{BG,bfuel}\right) - CCS\right) - \left(GSC + TP_{veg}\right)\right)$$

$$= -BSC + \Delta C_{AG,bfuel} + \Delta C_{BG,bfuel} + CCS + GSC + TP_{veg} \quad [8]$$

For simplicity, we define gross avoided fossil fuel emissions (AFFE) as the gasoline supply chain (GSC) and tail pipe (TP_{veg}) emissions displaced by biofuel use:

$$AFFE = GSC + TP_{veg} \quad [9]$$

Combining equations [8] and [9], we can express the net biophysical mitigation potential of the biofuel scenarios as the sum ecosystem carbon sequestration (or losses), geological carbon sequestration via CCS, and avoided fossil fuel emissions, minus biofuel supply chain emissions:

$$NM_{bfuel} = \Delta C_{AG,bfuel} + \Delta C_{BG,bfuel} + CCS + AFFE - BSC \quad [10]$$

Equations [8] and [10] are the basis for the GHG mitigation values reported in the text and in Figs. 3 & 4.

DayCent modeling

DayCent is a process-based ecosystem carbon, nitrogen, and water cycling model that simulates plant NPP, carbon partitioning, soil organic matter dynamics, and trace gas emissions on a daily time step (62). We used DayCent to estimate cellulosic biomass yields, changes in ecosystem carbon storage, and soil N_2O emissions (driven by synthetic nitrogen fertilizer application and other processes) for the various scenarios assessed. Our analysis focused on cropland and pasture transitioning out of agriculture and into either switchgrass cultivation or restoration of natural vegetation (grassland restoration or reforestation; see reforestation terminology note in Supplementary Information), as shown schematically in Fig. S2. Additional scenarios representing clear-cutting of secondary forest and conversion to switchgrass versus continued forest growth were also included for illustrative comparison with previous studies, e.g., Walker *et al.* 2010 (20).

Case study counties were selected as having significant amounts of both pasture land and row cropping as per informal visual inspection of the Cropland Data Layer (63); having climate conditions suitable for cropland, grassland or forest vegetation; and for having soils of diverse texture and ample depth as per the Soil Survey Geographic database (SSURGO) (64). Standard DayCent data inputs for soil texture and depth were derived from the SSURGO database, and weather inputs from the North American Regional Reanalysis database (65), as described previously in Field *et al.* 2016 (34). Within each case study the correlation between land quality and land use was represented by selecting a fine-textured soil (silt loam or similar) from among those present in the county to use for all simulations with a cropland initial condition, and a coarse-texture soil (sandy loam or similar) for simulations with pasture or forest initial condition, consistent with prior landscape-scale analysis (37).

Initialization of soil carbon and nitrogen levels was performed *via* simulation of pre-settlement land cover and historic land use consistent the EPA annual Inventory of U.S. Greenhouse Gas Emissions and Sinks (66). The resulting model initializations were then extended with 70-year forward simulations of biofuel feedstock production and ecosystem restoration scenarios as per Fig. S2. Additional details on post-processing raw DayCent simulation results to extract key ecosystem data (biomass harvest, changes in ecosystem carbon storage, NPP, R_h, and N_2O emissions) are available in the Supplementary Information. Accurate forward simulation requires both calibration of vegetation characteristics (tissue C:N ratio limits, temperature and moisture stress response, turnover of aboveground biomass and fine roots, and overall productivity potential (34)), and specification of management.

Our ‘current’ switchgrass simulations considered the lowland ecotype at the Louisiana case study site and upland switchgrass in Iowa and New York, based on the parameterization and simple model of switchgrass phenology as a function of latitude described in Field *et al.* 2016 (34). We assumed annual fertilizer application at a rate of 50 kg N ha^{-1}, annual biomass harvest (excluding the planting year), and field tilling and replanting every 10 years, and we adjusted switchgrass productivity down 15% to reflect deviations associated with scaling up field trial results to plantation scales (67). For the 'future' scenarios we set DayCent's switchgrass productivity potential parameter higher in order to achieve a 64% higher average biomass yield, equivalent to a 2% annual yield increase compounded over 25 years. This higher productivity was implemented at the beginning and held constant across the duration of the 70-year forward simulation. We note that maize yields in the US initially increased at an annual rate of 3.5–6% with the advent of concerted breeding and management improvement efforts in the 1930s, and were still increasing at an average rate of ~1.5% per year in the 1990s (68). Our simulated future mean switchgrass yield of 18.4 Mg ha^{-1} y^{-1} is within the range of current-day yields achievable across most of the eastern US with Miscanthus, energycane, and sorghum cultivated in their most appropriate respective environments (38).

We conservatively modeled our grassland restoration scenarios using the current-day switchgrass parameterization, but without nitrogen fertilizer application or harvest, and subject to light seasonal grazing. We created new regionally-specific parameterizations of native forest growth based on the forest yield tables in Smith *et al.* 2006 (35) for the New York ('Northeast' region in Smith *et al*. 2006), Iowa ('Northern Prairie States'), and Louisiana ('South Central') case study sites, adjusting symbiotic nitrogen fixation for broad consistency with soil total nitrogen trend data from two representative afforestation studies (69, 70). Additional details on forest parameter calibration are available in the Supplementary Information.

Biorefinery & CCS technology

Our 'current' cellulosic biofuel production scenario was modeled on the 'base' biochemical conversion pathway of dilute acid pre-treatment and simultaneous saccharification and fermentation to ethanol described in Laser *et al*. 2009 (40). This pathway is broadly consistent with the six pioneer commercial-scale cellulosic biorefineries that had been constructed worldwide as of 2017, with a combined nameplate annual production capacity of 450 million liters (58). Ethanol yield is estimated at 318 liters per dry metric tonne of biomass feedstock, or 40.4% of the energy content of the feedstock biomass (evaluated on a lower heating value, or LHV, basis). Recovered fermentation residues are combusted to power a Rankine cycle for generation of biorefinery process steam and electricity needs, with a net electricity export of 11.5 MW (2.9% of feedstock LHV).

Cellulosic ethanol production has only become a commercial reality during the last few years, and both experience-driven cost reductions within current processing paradigms and alternative processing paradigms with potential for large cost reductions and yield improvements are anticipated (71). We also considered a ‘future’ hybrid biochemical–thermochemical conversion case (72) based on ammonia fiber expansion pretreatment and consolidated bioprocessing to ethanol, followed by gasification of fermentation resides and single-pass Fischer-Tropsch (FT) conversion of the resulting syngas to gasoline- and diesel-weight FT liquids (41). This future case yields 54.1% of feedstock LHV as ethanol (440 L $(\text{Mg biomass})^{-1}$), 9.7% as FT diesel, and 6.1% as FT gasoline. The residual syngas not converted to FT liquids is combusted to produce biorefinery steam and electricity needs in a gas turbine combined cycle power island, with 5 MW (1.3%) net electricity export. Note that, in addition to the future increase in switchgrass yields discussed previously, the future conversion technology design assumes concurrent improvements in feedstock quality, specifically a 10% increase in carbohydrate content and 50% reduction in ash (40). The gasification process also produces a small amount of char, which we assume is soil-applied with 80% long-term carbon retention (73).

The future biorefinery design features a number of byproduct streams of high-purity CO_2 that are amenable to CCS. We used data from a coal- and biomass-to-liquids BECCS study with similar fuel yield assumptions (Liu *et al.* 2011) (74) to estimate CO_2 recovery rates and associated CCS parasitic energy requirements. The initial fermentation step in our future biorefinery produces CO_2 at a 1:1 stoichiometric ratio with ethanol, corresponding to 17.9% of input biomass carbon. Associated parasitic electricity requirement for gas dehydration, compression, and injection of that carbon dioxide were estimated at 27 MJ_e $(Mg\ CO_2)^{-1}$. During the subsequent thermochemical processing of fermentation residues, a syngas cleanup step improves once-through FT reactor yields while yielding an additional byproduct stream of CO_2. Liu *et al.* 2011 also considered autothermal reforming, water-gas shift, and CO_2 removal from the unconverted syngas downstream of the FT reactor prior to combustion. Together, these CO_2 streams comprise 30.2% of input biomass carbon, and we estimated an associated CCS parasitic energy requirement of 75 MJ_e $(Mg\ CO_2)^{-1}$ for the additional separation, dehydration, compression, and injection steps. Full biorefinery carbon balances are detailed in Table S1.

Supply chain emissions & displacement factors

Life cycle emissions associated with farm inputs, on-farm energy use, farm–biorefinery transport, and biorefinery inputs were estimated using the Argonne National Laboratory Greenhouse Gases, Regulated Emissions, and Energy Use in Transportation (GREET) life cycle assessment model (75), specifically GREET 2018 database version 13395. GREET evaluates the life cycle 100-year global warming potential (GWP_{100}) from CO_2 and other GHGs (e.g., methane and N_2O) and climate forcing agents (e.g., black carbon) for different transportation technologies and their associated technosphere inputs. Farm inputs and energy use rates were modified within the ‘switchgrass production for ethanol plant’ pathway based on a previously published model of switchgrass cultivation (37). That model includes per-area estimates of farm operation diesel fuel use and nutrient, herbicide, and lime application, as well as estimates of harvest operation fuel use and nutrient replacement requirements on a per-ton-biomass-harvested basis. We retained the GREET default assumption for switchgrass farm–biorefinery transport of 106 km (one-way) *via* heavy-duty truck. The field-to-biorefinery-gate footprint associated with these inputs and energy use was then evaluated in GREET over a range of switchgrass per-area yield assumptions, enabling us to fit a simple model (power regression) of that footprint as a continuous function of yield, which could be integrated into our python code and applied to our DayCent-derived yield estimates (Fig. S6). For simplicity, the same life cycle emissions footprint model was also applied to wood harvested in scenarios of secondary forest conversion to switchgrass, and we assumed that feedstock would also be processed *via* the same biorefinery process described in the previous section.

Most biorefinery process energy and electricity requirements are met through combustion of conversion byproducts. However, other biorefinery inputs include sulfuric acid and/or ammonia for biomass pretreatment, lime for process pH control, corn steep liquor for fermentation organism nutrients, and water to make up losses from WWT and elsewhere in the system. These inputs were estimated from Laser *et al.* 2009 (40) Tables 12 & 13 subject to a 0.5% mass cut-off rule (excluding make-up water mass from that total) and used to adjust the default GREET ‘coproduction of ethanol and power from switchgrass’ pathway. Liquid biofuels and electricity produced by our simulated biorefinery were assumed to displace conventional gasoline, diesel, and US mix grid electricity on a 1:1 energy basis (see Fig. 2, noting that electricity co-production is omitted there for simplicity). The well-to-wheel life cycle emissions footprint of each megajoule of conventional fuel (including both tailpipe emissions and upstream emissions associated with petroleum extraction and refining) or grid electricity displaced were estimated using emissions factors extracted from GREET, evaluated in the year 2019 for the 'current' bioenergy scenario and in 2044 for the 'future' scenario. Note that the biorefineries in both of those scenarios are net electricity exporters, though the addition of CCS in the 'future' scenario tips the biorefinery over to a small electricity importer (Table S1).

Literature estimates of total induced LUC

Pavlenko & Searle 2018 (44) compiled a survey of prior literature total induced LUC estimates for switchgrass, Miscanthus, and unspecified perennial energy grasses made using a variety of global agricultural trade models. The EPA used the FASOM-FAPRI model to estimate LUC emissions associated with 30 gigaliters (GL y^{-1}) of annual cellulosic ethanol production from switchgrass feedstocks, as detailed in their regulatory impact analysis for the US renewable fuel standard (76). Plevin & Mishra conducted a similar analysis using the GCAM model considering 34 GL y^{-1} of switchgrass ethanol production (77). The GTAP model has been used to predict the land use response to 27 GL y^{-1} of ethanol production from either switchgrass or Miscanthus feedstocks (78). Multiple teams have subsequently applied different ecosystem carbon stock estimates to those results in order to estimate LUC emissions (45, 79, 80). Finally, Valin *et al.* used the GLOBIOM model to consider the LUC impacts of cellulosic ethanol production from perennial grass cultivation in Europe (81).

Together these comprise 9 estimates of total induced LUC impacts for the large-scale production of cellulosic ethanol from dedicated perennial energy grasses, assessed using 4 different economic models. Those LUC modeling results are detailed in Table S2, using the sign convention that positive values denote net emissions to atmosphere and negative denotes net sequestration. LUC estimates are typically reported on a fuel basis in units of g CO_2e MJ^{-1}. In order to convert these estimates to a per-area basis for comparison with the rest of our analysis, we used the total biofuel production rate, energy crop yield, and total direct land use values assumed or predicted in each study (as compiled by Pavlenko & Searle 2018 (44)) to back-calculate the ethanol yield per tonne of cellulosic biomass, and then express the per-MJ total induced LUC results on a per-ha basis (Mg CO_2e ha^{-1} y^{-1}) instead. Insufficient information was reported for the GLOBIOM model to back-calculate the per-Mg-biomass fuel yield, so we used the average value across the other studies in that case.

The international land use change component of total induced land use change was broken out for 6 of the 9 sets of LUC results examined (44, 45). We converted those results from a per-MJ to a per-ha basis in the same manner as above. These data provide an alternate point of comparison for our direct mitigation estimates, since they isolate international market-mediated agricultural extensification and intensification effects (which we did not assess in our modeling), excluding the confounding (and often compensatory) effect of direct soil carbon sequestration on the land where those crops are cultivated (which is already included in our assessment).

Data availability

The DayCent model (https://www2.nrel.colostate.edu/projects/daycent/) is freely available upon request. Specification of DayCent model runs and automated model initialization, calibration, scenario simulation, results analysis, and figure generation were implemented in Python 2.7, using the *numpy* module for data processing and the *matplotlib* module for figure generation. Analysis code is available in a version-controlled repository (https://github.com/johnlfield/Ecosystem_dynamics). A working copy of the code, all associated DayCent model inputs, and analysis outputs are also available in an online data repository (https://figshare.com/s/4c14ec168bd550db4bad; note this URL is for accessing a private version of the repository, and will eventually be replaced with an updated URL for the public version of the repository, which will only be accessible after the journal-specified embargo date).

ACKNOWLEDGEMENTS

We thank Dennis Ojima and Daniel L. Sanchez for their encouragement on this topic. The authors gratefully acknowledge partial support as follows: J.L.F., L.R.L., T.L.R., E.A.H.S., and J.J.S., the Sao Paulo Research Foundation (FAPESP grant# 2014/26767-9); J.L.F., L.R.L., K.P., and T.L.R., The Center for Bioenergy Innovation, a U.S. Department of Energy Research Center supported by the Office of Biological and Environmental Research in the DOE Office of Science (grant# DE-AC05-00OR22725); L.R.L., the Sao Paulo Research Foundation, and the Link Foundation; J.L.F. and K.P., USDA/NIFA (grant# 2013-68005-21298 and 2017-67019-26327); T.L.R., USDA/NIFA (grant# 2012-68005-19703); D.S.L. and S.P.L., the Energy Biosciences Institute.

AUTHOR CONTRIBUTIONS

L.R.L., T.L.R., and E.A.H.S. conceptualized the study; J.L.F. performed the formal analysis and results visualization; L.R.L. and J.J.S. acquired funding to support the work; E.A.H.S. and K.P. developed the ecosystem modeling methodology; T.L.R. and M.S.L. developed the biofuel production and carbon capture and storage technology modeling methodology; L.R.L., H.C., Z.Q. and M.Q.L.W. developed the methodology for providing comparative estimates of induced land use change; J.L.F. and L.R.L. produced the original manuscript draft; D.S.L., S.P.L., P.S. and all other listed co-authors contributed to manuscript review and editing.

COMPETING INTERESTS

The Energy Biosciences Institute was funded by BP America.

REFERENCES

1. J. G. Canadell, E. D. Schulze, Global potential of biospheric carbon management for climate mitigation. *Nature Communications* **5**, 5282 (2014).
2. D. P. van Vuuren, *et al.*, Alternative pathways to the 1.5 °C target reduce the need for negative emission technologies. *Nature Climate Change* **8**, 391–397 (2018).
3. J. Rogelj, D. Shindell, K. Jiang, "Chapter 2: Mitigation pathways compatible with 1.5°C in the context of sustainable development" in *Global Warming of 1.5 °C*, (UN Intergovernmental Panel on Climate Change, 2018) (October 11, 2018).

4. L. M. Fulton, L. R. Lynd, A. Körner, N. Greene, L. R. Tonachel, The need for biofuels as part of a low carbon energy future. *Biofuels, Bioproducts and Biorefining* **9**, 476–483 (2015).
5. S. J. Davis, *et al.*, Net-zero emissions energy systems. *Science* **360**, eaas9793 (2018).
6. D. Tilman, J. Hill, C. Lehman, Carbon-negative biofuels from low-input high-diversity grassland biomass. *Science* **314**, 1598–1600 (2006).
7. S. Fuss, *et al.*, Betting on negative emissions. *Nature Climate Change* **4**, 850–853 (2014).
8. J. Lehmann, A handful of carbon. *Nature* **447**, 143–144 (2007).
9. D. L. Sanchez, N. Johnson, S. T. McCoy, P. A. Turner, K. J. Mach, Near-term deployment of carbon capture and sequestration from biorefineries in the United States. *Proceedings of the National Academy of Sciences* **115**, 4875–4880 (2018).
10. P. A. Turner, C. B. Field, D. B. Lobell, D. L. Sanchez, K. J. Mach, Unprecedented rates of land-use transformation in modelled climate change mitigation pathways. *Nature Sustainability* **1**, 240–245 (2018).
11. T. L. Richard, Challenges in scaling up biofuels infrastructure. *Science* **329**, 793–796 (2010).
12. A. E. Farrell, *et al.*, Ethanol can contribute to energy and environmental goals. *Science* **311**, 506–508 (2006).
13. J. Fargione, J. Hill, D. Tilman, S. Polasky, P. Hawthorne, Land clearing and the biofuel carbon debt. *Science* **319**, 1235–1238 (2008).
14. T. Searchinger, *et al.*, Use of US croplands for biofuels increases greenhouse gases through emissions from land-use change. *Science* **319**, 1238–1240 (2008).

15. A. Zumkehr, J. E. Campbell, Historical U.S. cropland areas and the potential for bioenergy production on abandoned croplands. *Environmental Science & Technology* **47**, 3840–3847 (2013).

16. I. Gelfand, *et al.*, Sustainable bioenergy production from marginal lands in the US Midwest. *Nature* **493**, 514–517 (2013).

17. A. Lamb, *et al.*, The potential for land sparing to offset greenhouse gas emissions from agriculture. *Nature Climate Change* **6**, 488–492 (2016).

18. D. Tilman, M. Clark, Global diets link environmental sustainability and human health. *Nature* **515**, 518–522 (2014).

19. R. Righelato, D. V. Spracklen, Carbon mitigation by biofuels or by saving and restoring forests? *Science* **317**, 902–902 (2007).

20. T. Walker, *et al.*, Biomass sustainability and carbon policy study. *Manomet Center for Conservation Sciences* (2010) (August 10, 2019). www.manomet.org/wp-content/uploads/2018/03/Manomet_Biomass_Report_Full_June2010.pdf

21. J. F. Beckman, Samuel Evans, Ronald D. Sands, U.S. Renewable Fuel Standard 2: Impacts of Cellulosic Biofuel Production in (2011). Paper at the Agricultural and Applied Economics Association 2011 AAEA & NAREA Joint Annual Meeting, Pittsburgh, PA. https://ageconsearch.umn.edu/record/103751/

22. H. Haberl, Net land-atmosphere flows of biogenic carbon related to bioenergy: towards an understanding of systemic feedbacks. *GCB Bioenergy* **5**, 351–357 (2013).

23. S. L. Lewis, C. E. Wheeler, E. T. A. Mitchard, A. Koch, Restoring natural forests is the best way to remove atmospheric carbon. *Nature* **568**, 25 (2019).

24. T. D. Searchinger, T. Beringer, A. Strong, Does the world have low-carbon bioenergy potential from the dedicated use of land? *Energy Policy* **110**, 434–446 (2017).

25. J. M. DeCicco, W. H. Schlesinger, Opinion: Reconsidering bioenergy given the urgency of climate protection. *Proceedings of the National Academy of Sciences* **115**, 9642–9645 (2018).

26. J. M. DeCicco, Biofuel's carbon balance: doubts, certainties and implications. *Climatic Change* **121**, 801–814 (2013).

27. J. M. DeCicco, *et al.*, Carbon balance effects of U.S. biofuel production and use. *Climatic Change* **138**, 667–680 (2016).

28. T. Searchinger, Biofuels and the need for additional carbon. *Environmental Research Letters* **5**, 024007 (2010).

29. H. Haberl, *et al.*, Correcting a fundamental error in greenhouse gas accounting related to bioenergy. *Energy Policy* **45**, 18–23 (2012).

30. F. S. Chapin, *et al.*, Reconciling carbon-cycle concepts, terminology, and methods. *Ecosystems* **9**, 1041–1050 (2006).

31. M. Abraha, I. Gelfand, S. K. Hamilton, J. Chen, G. P. Robertson, Carbon debt of field-scale conservation reserve program grasslands converted to annual and perennial bioenergy crops. *Environmental Research Letters* **14**, 024019 (2019).

32. T. Zenone, I. Gelfand, J. Chen, S. K. Hamilton, G. P. Robertson, From set-aside grassland to annual and perennial cellulosic biofuel crops: Effects of land use change on carbon balance. *Agricultural and Forest Meteorology* **182–183**, 1–12 (2013).

33. S. J. Del Grosso, W. J. Parton, C. A. Keough, M. Reyes-Fox, "Special features of the DayCent modeling package and additional procedures for parameterization, calibration,

validation, and applications" in *Advances in Agricultural Systems Modeling*, Methods of introducing system models into agricultural research., L. R. Ahuja, L. Ma, Eds. (American Society of Agronomy, Crop Science Society of America, Soil Science Society of America, 2011), pp. 155–176.

34. J. L. Field, E. Marx, M. Easter, P. R. Adler, K. Paustian, Ecosystem model parameterization and adaptation for sustainable cellulosic biofuel landscape design. *GCB Bioenergy* **8**, 1106–1123 (2016).
35. J. E. Smith, L. S. Heath, K. E. Skog, R. A. Birdsey, Methods for calculating forest ecosystem and harvested carbon with standard estimates for forest types of the United States (2006) (November 22, 2016). http://www.treesearch.fs.fed.us/pubs/22954
36. C. C. Brandt, *et al.*, "2016 Billion-Ton Report: Advancing domestic resources for a thriving bioeconomy, Volume 1: Economic availability of feedstocks" (Oak Ridge National Lab. (ORNL), Oak Ridge, TN (United States), 2016) https:/doi.org/10.2172/1435342 (October 20, 2018).
37. J. L. Field, *et al.*, High-resolution techno–ecological modelling of a bioenergy landscape to identify climate mitigation opportunities in cellulosic ethanol production. *Nature Energy* **3**, 211–219 (2018).
38. D. K. Lee, *et al.*, Biomass production of herbaceous energy crops in the United States: field trial results and yield potential maps from the multiyear regional feedstock partnership. *GCB Bioenergy* **10**, 698–716 (2018).
39. D. Baldocchi, J. Penuelas, The physics and ecology of mining carbon dioxide from the atmosphere by ecosystems. *Global Change Biology* **25**, 1191–1197 (2019).

40. M. Laser, H. Jin, K. Jayawardhana, L. R. Lynd, Coproduction of ethanol and power from switchgrass. *Biofuels, Bioproducts and Biorefining* **3**, 195–218 (2009).
41. M. Laser, H. Jin, K. Jayawardhana, B. E. Dale, L. R. Lynd, Projected mature technology scenarios for conversion of cellulosic biomass to ethanol with coproduction thermochemical fuels, power, and/or animal feed protein. *Biofuels, Bioproducts and Biorefining* **3**, 231–246 (2009).
42. S. G. Evans, B. S. Ramage, T. L. DiRocco, M. D. Potts, Greenhouse gas mitigation on marginal land: A quantitative review of the relative benefits of forest recovery versus biofuel production. *Environmental Science & Technology* **49**, 2503–2511 (2015).
43. U.S. Environmental Protection Agency, "Framework for assessing biogenic CO2 emissions from stationary sources" (2014) (August 10, 2019). https://yosemite.epa.gov/sab/sabproduct.nsf/0/3235DAC747C16FE985257DA90053F252/$File/Framework-for-Assessing-Biogenic-CO2-Emissions+(Nov+2014).pdf
44. N. Pavlenko, S. Searle, "A comparison of induced land-use change emissions estimates from energy crops" (The International Council on Clean Transportation, 2018) (August 10, 2019). https://theicct.org/publications/comparison-ILUC-emissions-estimates-energy-crops
45. Z. Qin, J. B. Dunn, H. Kwon, S. Mueller, M. M. Wander, Influence of spatially dependent, modeled soil carbon emission factors on life-cycle greenhouse gas emissions of corn and cellulosic ethanol. *GCB Bioenergy* **8**, 1136–1149 (2016).
46. 110th Congress of the United States, Energy Independence and Security Act of 2007 (2007).
47. D. Rajagopal, G. Hochman, D. Zilberman, Indirect fuel use change (IFUC) and the lifecycle environmental impact of biofuel policies. *Energy Policy* **39**, 228–233 (2011).

48. E. Smeets, *et al.*, The impact of the rebound effect of the use of first generation biofuels in the EU on greenhouse gas emissions: A critical review. *Renewable and Sustainable Energy Reviews* **38**, 393–403 (2014).
49. R. York, Do alternative energy sources displace fossil fuels? *Nature Climate Change* **2**, 441–443 (2012).
50. M. Norton, *et al.*, Serious mismatches continue between science and policy in forest bioenergy. *GCB Bioenergy* **11**, 1256–1263 (2019).
51. W. H. Schlesinger, Are wood pellets a green fuel? *Science* **359**, 1328–1329 (2018).
52. A. B. Harper, *et al.*, Land-use emissions play a critical role in land-based mitigation for Paris climate targets. *Nature Communications* **9**, 2938 (2018).
53. P. Dass, B. Z. Houlton, Y. Wang, D. Warlind, Grasslands may be more reliable carbon sinks than forests in California. *Environmental Research Letters* **13**, 074027 (2018).
54. J. F. Bastin, *et al.*, The global tree restoration potential. *Science* **365**, 76–79 (2019).
55. O. Cintas, *et al.*, The potential role of forest management in Swedish scenarios towards climate neutrality by mid century. *Forest Ecology and Management* **383**, 73–84 (2017).
56. G. P. Robertson, *et al.*, Cellulosic biofuel contributions to a sustainable energy future: Choices and outcomes. *Science* **356**, eaal2324 (2017).
57. C. Robledo-Abad, *et al.*, Bioenergy production and sustainable development: science base for policymaking remains limited. *GCB Bioenergy* **9**, 541–556 (2017).
58. L. R. Lynd, *et al.*, Cellulosic ethanol: status and innovation. *Current Opinion in Biotechnology* **45**, 202–211 (2017).
59. D. M. Reiner, Learning through a portfolio of carbon capture and storage demonstration projects. *Nature Energy* **1**, 15011 (2016).

60. C. K. Wright, B. Larson, T. J. Lark, H. K. Gibbs, Recent grassland losses are concentrated around U.S. ethanol refineries. *Environmental Research Letters* **12**, 044001 (2017).

61. G. M. Lovett, J. J. Cole, M. L. Pace, Is net ecosystem production equal to ecosystem carbon accumulation? *Ecosystems* **9**, 152–155 (2006).

62. W. J. Parton, M. Hartman, D. Ojima, D. Schimel, DAYCENT and its land surface submodel: Description and testing. *Global and Planetary Change* **19**, 35–48 (1998).

63. C. Boryan, Z. Yang, R. Mueller, M. Craig, Monitoring US agriculture: the US Department of Agriculture, National Agricultural Statistics Service, Cropland Data Layer Program. *Geocarto International* **26**, 341–358 (2011).

64. D. J. Ernstrom, D. Lytle, Enhanced soils information systems from advances in computer technology. *Geoderma* **60**, 327–341 (1993).

65. F. Mesinger, *et al.*, North American Regional Reanalysis. *Bulletin of the American Meteorological Society* **87**, 343–360 (2006).

66. US EPA, “Inventory of U.S. greenhouse gas emissions and sinks: 1990-2012” (US Environmental Protection Agency, 2014) (March 17, 2014). http://www.epa.gov/climatechange/ghgemissions/usinventoryreport.html

67. S. Y. Searle, C. J. Malins, Will energy crop yields meet expectations? *Biomass and Bioenergy* **65**, 3–12 (2014).

68. S. B. McLaughlin, J. R. Kiniry, C. M. Taliaferro, D. De La Torre Ugarte, “Projecting yield and utilization potential of switchgrass as an energy crop” in *Advances in Agronomy*, (Academic Press, 2006), pp. 267–297.

69. J. M. H. Knops, D. Tilman, Dynamics of soil nitrogen and carbon accumulation for 61 years after agricultural abandonment. *Ecology* **81**, 88–98 (2000).

70. E. A. Paul, S. J. Morris, J. Six, K. Paustian, E. G. Gregorich, Interpretation of soil carbon and nitrogen dynamics in agricultural and afforested soils. *Soil Science Society of America Journal* **67**, 1620–1628 (2003).
71. L. R. Lynd, The grand challenge of cellulosic biofuels. *Nature Biotechnology* **35**, 912–915 (2017).
72. M. Laser, *et al.*, Comparative analysis of efficiency, environmental impact, and process economics for mature biomass refining scenarios. *Biofuels, Bioproducts and Biorefining* **3**, 247–270 (2009).
73. K. G. Roberts, B. A. Gloy, S. Joseph, N. R. Scott, J. Lehmann, Life cycle assessment of biochar systems: estimating the energetic, economic, and climate change potential. *Environmental Science & Technology* **44**, 827–833 (2010).
74. G. Liu, E. D. Larson, R. H. Williams, T. G. Kreutz, X. Guo, Making Fischer−Tropsch fuels and electricity from coal and biomass: performance and cost analysis. *Energy Fuels* **25**, 415–437 (2011).
75. M. Wang, M. Wu, H. Huo, Life-cycle energy and greenhouse gas emission impacts of different corn ethanol plant types. *Environmental Research Letters* **2**, 024001 (2007).
76. U. S. Environmental Protection Agency, Assessment and Standards Division, Office of Transportation and Air Quality, Renewable fuel standard program (RFS2) regulatory impact analysis. *United States Environmental Protection Agency, Washington, DC* (2010). https://nepis.epa.gov/Exe/ZyPURL.cgi?Dockey=P1006DXP.TXT
77. R. Plevin, G. Mishra, Estimates of the land-use-change carbon intensity of ethanol from switchgrass and corn stover using the GCAM 4.0 model. *Report to Environmental Working Group* (2015). http://static.ewg.org/reports/2015/better-biofuels-ahead/plevinreport.pdf

78. F. Taheripour, W. E. Tyner, M. Q. Wang, Global land use changes due to the US cellulosic biofuel program simulated with the GTAP model. *Argonne National Laboratory* (2011). https://greet.es.anl.gov/publication-luc_ethanol

79. J. B. Dunn, S. Mueller, H. Kwon, M. Q. Wang, Land-use change and greenhouse gas emissions from corn and cellulosic ethanol. *Biotechnology for Biofuels* **6**, 51 (2013).

80. F. Taheripour, W. E. Tyner, Induced land use emissions due to first and second generation biofuels and uncertainty in land use emission factors. *Economics Research International* **2013**, 1–12 (2013).

81. H. Valin, *et al.*, "The land use change impact of biofuels consumed in the EU: Quantification of area and greenhouse gas impacts" (2015) (March 11, 2019). https://ec.europa.eu/energy/sites/ener/files/documents/Final%20Report_GLOBIOM_publication.pdf

82. T. W. Hudiburg, B. E. Law, C. Wirth, S. Luyssaert, Regional carbon dioxide implications of forest bioenergy production. *Nature Climate Change* **1**, 419–423 (2011).

83. H. G. Lund, *Definitions of forest, deforestation, afforestation, and reforestation (2014 rev*)* (Forest Information Services, 2014). http://home.comcast.net/~gyde/DEFpaper.htm

84. J. W. Veldman, *et al.*, Tyranny of trees in grassy biomes. *Science* **347**, 484–485 (2015).

85. N. Seddon, B. Turner, P. Berry, A. Chausson, C. A. J. Girardin, Grounding nature-based climate solutions in sound biodiversity science. *Nature Climate Change* **9**, 84 (2019).

86. G. Popkin, How much can forests fight climate change? *Nature* **565**, 280 (2019).

87. X. Liu, T. Yang, Q. Wang, F. Huang, L. Li, Dynamics of soil carbon and nitrogen stocks after afforestation in arid and semi-arid regions: A meta-analysis. *Science of The Total Environment* **618**, 1658–1664 (2018).

88. L. Deng, Z. Shangguan, Afforestation drives soil carbon and nitrogen changes in China. *Land Degradation & Development* **28**, 151–165 (2017).

89. D. Li, S. Niu, Y. Luo, Global patterns of the dynamics of soil carbon and nitrogen stocks following afforestation: a meta-analysis. *New Phytologist* **195**, 172–181 (2012).

90. J. B. Dunn, *et al.*, "Supply chain sustainability analysis of three biofuel pathways" (Idaho National Laboratory (INL), 2013) (December 1, 2016). http://www.osti.gov/scitech/biblio/1149014

FIGURE LEGENDS

Fig. 1. Modeled ecosystem carbon fluxes for different land use scenarios. Stacked bar plot showing DayCent estimates of ecosystem carbon inputs *via* net primary production (NPP, pink bars) and total carbon losses *via* both heterotrophic respiration (R_h, white bars) and harvest (Harv) of switchgrass (blue bars) and wood (green bars) for biofuel production for the New York (NY), Iowa (IA), and Louisiana (LA) case studies. The resulting net ecosystem carbon balance (NECB) is marked with green diamonds, with positive values indicating increases in ecosystem carbon storage. The results are annual averages across the first 30 years of simulation.

Fig. 2. Modeled atmosphere–biosphere–geosphere carbon flows. Flows of carbon between the atmosphere (blue), biosphere (green), and geosphere (black) in gaseous (dotted lines) and solid or liquid (solid lines) forms, for biofuel/BECCS scenarios ('bfuel', **A**), or restoration or retention of natural vegetation ('veg', **B**). Geosphere-derived fossil carbon fluxes (black) include biofuel supply chain emissions (BSC) in the bioenergy scenarios, and gasoline supply chain emissions (GSC) and tailpipe emissions (TP_{veg}) in the vegetation scenarios. Flows of biosphere-derived biogenic carbon (green) include net primary production (NPP), heterotrophic respiration (R_h), biomass harvest (Harv), biofuel combustion tailpipe emissions (TP_{bfuel}), and biorefinery emissions of by-product CO_2 (BP), which in the BECCS scenario are diverted into geological storage *via* carbon capture and storage (CCS).

Fig. 3. Cumulative biophysical GHG mitigation potential versus time. Results plotted individually for the three test sites under scenarios of (**A**) biofuel production on former

agricultural land, (**B**) natural vegetation restoration on former agricultural land, and (**C**) secondary forest harvest and conversion to biofuel production versus continued undisturbed growth. Displacement of fossil fuel emissions by biofuel production and carbon sequestration in ecosystems or *via* CCS are positive mitigation; newly incurred supply chain fossil fuel emissions and ecosystem carbon losses are negative. The fine saw-tooth pattern is driven by seasonal cycles of biomass growth and harvest.

Fig. 4. Net GHG mitigation potential for biofuel/BECCS and vegetation restoration/retention scenarios. Results are annual averages across the first 30 years of simulation, for direct mitigation effects only (no ILUC or other indirect effects included). Net biophysical mitigation potential includes changes in above- and belowground ecosystem carbon storage, avoided fossil fuel emissions (AFFE) from the displacement of conventional fuel use by biofuel production, biogenic carbon capture and storage (CCS), and biofuel supply chain emissions (BSC) including fertilizer-derived soil nitrous oxide emissions. Avoided emissions and carbon sequestration are positive mitigation; new fossil emissions or net losses of ecosystem carbon storage are negative. Markers show the average net mitigation potential across the three case study sites, and error bars denote the range. Quantitative flow diagrams illustrate the average carbon fluxes in representative reforestation (**B**) and BECCS (**C**) scenarios. To reduce visual clutter in panel **C**, a small (1.5 Mg CO_2 ha^{-1} y^{-1}) biofuel production (BP) emission is combined into the TP_{bfuel} term, BSC emissions (1.2 Mg CO_2 ha^{-1} y^{-1}, excluding N_2O) are subtracted out from the AFFE term, and the CCS term includes a small (0.5 Mg CO_2 ha^{-1} y^{-1}) component representing carbon sequestration as gasification char by-product applied to soils.

Fig. 5. Literature estimates of total induced land use change (LUC) compared to the system design factors assessed here. LUC emissions estimates are adapted from those compiled in Pavlenko & Searle 2018 (44) and from the Argonne National Laboratory CCLUB model (45). Biofuel system design factors consist of targeted feedstock production on cropland and avoidance of secondary forest conversion, switchgrass yield and biofuel conversion technology improvements, and sequestration of the biorefinery CO_2 byproduct *via* CCS. Land conversion choices are evaluated in terms of differences in total per-hectare net mitigation (NM) potential from cropland, pasture, or secondary forest conversion to biofuel production. Error bars denote the full range of results across all relevant analysis scenarios and case study sites.

FIGURES

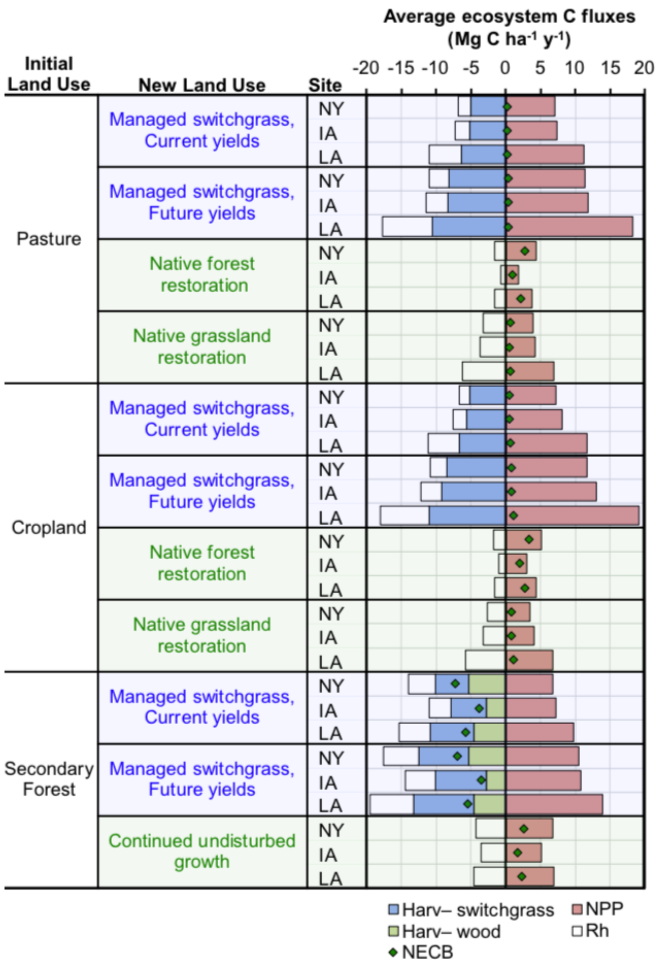

Fig. 1. (1 column wide)

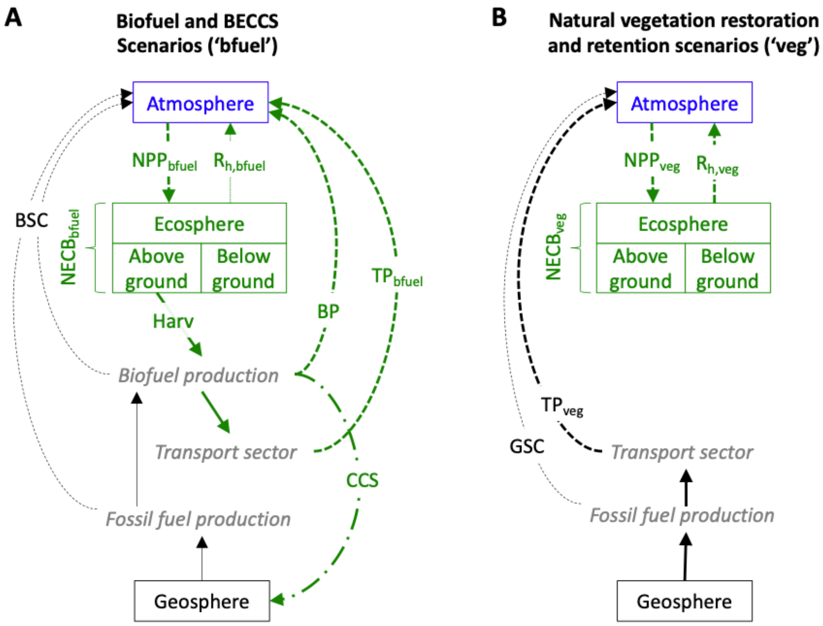

Fig. 2. (1.5 columns wide)

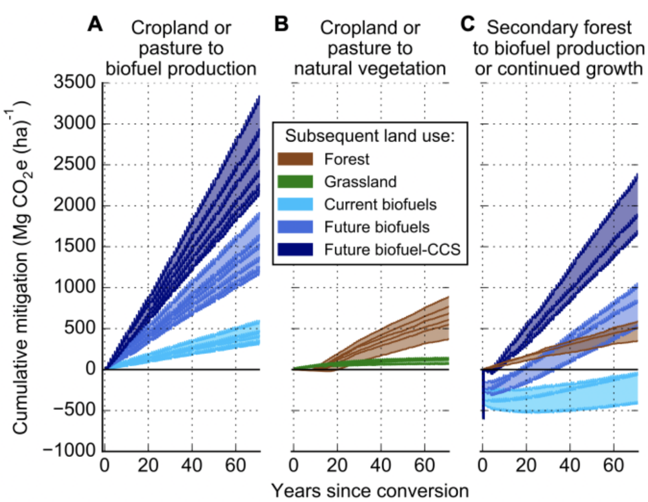

Fig. 3. (1 column wide)

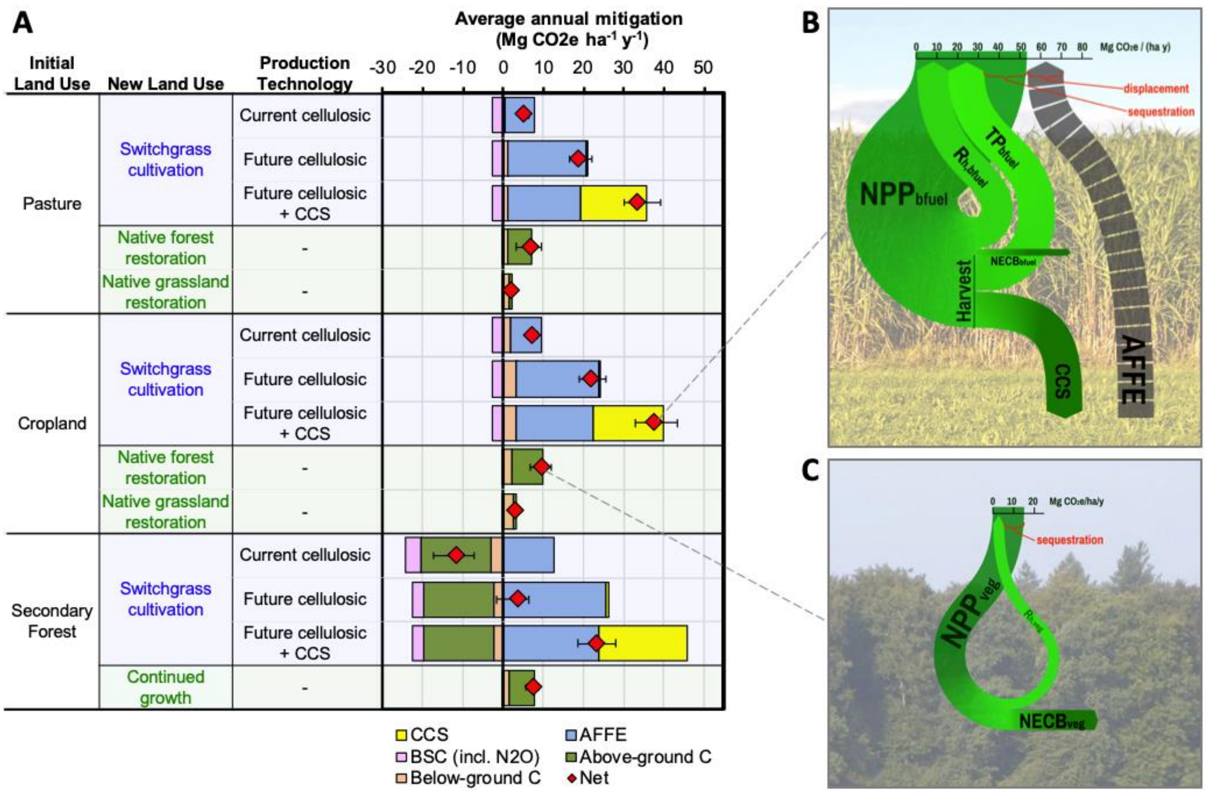

Fig. 4. (2 columns wide)

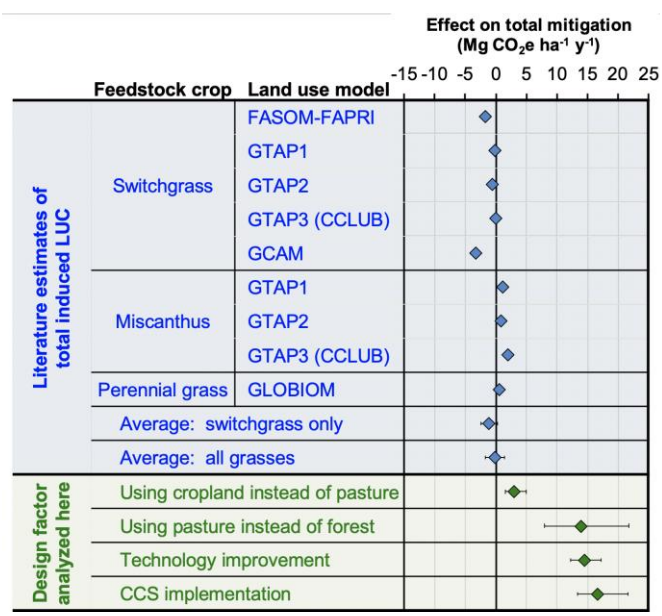

Fig. 5. (1 column wide)

SUPPORTING INFORMATION

Ecosystem carbon accounting conventions

We used the metric of net ecosystem carbon balance (NECB) as defined in Chapin *et al.* 2006 (30), and equations presented in Lovett *et al.* 2006 (61) to represent changes in ecosystem carbon storage over time. It is common for bioenergy greenhouse gas (GHG) accounting studies to focus on soil organic matter (SOM) as the primary indicator of long-term changes in ecosystem carbon storage. In conventional agricultural systems SOM is the largest, most stable, and most integrative carbon pool, whereas carbon in surface vegetation and litter is often ignored as a smaller and more transient pool that fluctuates greatly over the course of a growing season (37). However, the current analysis considered more extensive land use changes including reforestation and grassland restoration, and thus required more extensive ecosystem carbon accounting capable of representing changes in aboveground woody and herbaceous biomass in addition to belowground storage.

Assuming that there are no significant inputs or outputs of *inorganic* carbon in our agricultural and forested systems of interest, we used Eqns. 2 & 3 from Lovett *et al.* 2006 to represent a simple mass balance for *organic* carbon:

$$\Delta C_{org} = GPP + I - R_e - Ox_{nb} - E$$

where changes in ecosystem organic carbon storage reflect the balance between organic carbon inputs from gross primary production (GPP, the total rate of C fixation by photosynthesis) and other inputs (I), and losses from ecosystem respiration (R_e, the sum of autotrophic respiration R_a and heterotrophic respiration R_h), non-biotic oxidation of organic carbon due to fire and ultraviolet oxidation (Ox_{nb}), and other exports of carbon from the system (E).

The total change in ecosystem organic carbon storage is equivalent to NECB in systems where inorganic carbon fluxes are negligible, as per Eqn. 1 in Chapin *et al.* 2006. This change can be further divided into aboveground (ΔC_{AG}) and belowground (ΔC_{BG}) components for accounting convenience. We assumed that lateral inputs of organic carbon from outside the boundary of our agricultural and forested systems are minimal, that losses from fire and non-biotic oxidation are negligible, and that the only significant export of organic carbon from our systems is harvest of biomass (Harv). We therefore simplified our governing equation to:

$$NECB = \Delta C_{AG} + \Delta C_{BG} = GPP - R_e - Harv$$

GPP in terrestrial ecosystems is typically evaluated via eddy flux towers or other direct gas exchange measurements. However, DayCent and many other ecosystem models simulate net primary production, the difference between GPP and autotrophic respiration ($NPP=GPP–R_a$). We therefore re-wrote our ecosystem carbon storage governing equation for better compatibility with ecosystem model outputs as:

$$NECB = \Delta C_{AG} + \Delta C_{BG} = NPP - R_h - Harv$$

Integrating these carbon balance estimates over large spatial and temporal scales in order to account for landscape heterogeneity, disturbance, and interactions between the two is often termed net biome production (NBP) (30). NBP has been used previously to estimate spatially continuous long-term forest carbon storage trends at regional scales where inventory data is plentiful (82). However, our analysis was spatially discreet, and thorough accounting for different possible future disturbance regimes was outside the scope of the current work.

Reforestation terminology

The terms 'reforestation' and 'afforestation' are often invoked together or used interchangeably, and their technical definitions across the scientific and regulatory literature are varied and highly overlapping (83). Our analysis considered bioenergy production as an alternative to lightly-managed or unmanaged restoration of natural vegetation on former agricultural land, for example the historical abandonment of cropland in New England or more recent establishment of conservation easements on marginal or degraded land. Many of the definitions cited in Lund 2014 (83) and other papers cited in our work (e.g., Smith *et al.* 2006 (35)) would use the term afforestation for such cases, as these lands were put into agriculture long ago and have not recently been classified as forest. However, in the context of climate mitigation and carbon dioxide removal the term afforestation is often invoked for the highly-managed establishment of forest on lands that were not previously forested with the explicit goal of sequestering carbon (84). This can involve intensive site preparation or application of fertilizer or irrigation to promote tree establishment, or the planting of non-native higher-productivity species to increase sequestration rates. Such schemes can produce high initial rates of carbon sequestration, though at the expense of less biodiversity value and possibly reduced resilience to future disturbance (85).

Our mitigation-focused analysis considered secondary succession of regionally appropriate forest types, and as such we used the term reforestation to differentiate from that more targeted, active forest establishment and management for carbon sequestration (84). The ultimate biophysical mitigation potential of such active afforestation depends on tree selection, management choices, and the vulnerability of the resulting system to wildfire and other natural disturbances. A thorough analysis and quantification of these factors was outside the scope of the current work. Rather, our case study sites were selected to be representative of reforestation following agricultural abandonment in regions where forest was historically the dominant land cover (Wayne County, New York) or within the historic forest–grassland transition zone (Webster County, Iowa, and La Salle Parish, Louisiana) where both land covers would have been common and disturbance frequent. These sites also avoid boreal and montane forests in which countervailing biophysical warming effects (e.g., albedo increases) may offset much of the climate mitigation value of carbon sequestration (86).

DayCent simulation post-processing

DayCent estimates NPP as a dynamic function of insolation (based on latitude and weather conditions), soil temperature and moisture, canopy development (affects light interception), soil mineral nitrogen availability, and root zone development (affects ability of plant to access moisture and nitrogen in deeper soil layers) (33). Carbon partitioning between shoots and roots is dynamically adjusted based on simulated plant moisture and nutrient stress status. Soil organic carbon (SOC) dynamics reflect the rate of carbon inputs from aboveground litter and fine root turnover, and their transfer between three conceptual SOC pools (‘active’, ‘slow’, and ‘passive’) with different intrinsic turnover times. Actual turnover rates are dynamically adjusted for soil moisture and temperature, and carbon stabilization efficiency is determined as a function of soil texture and plant litter chemistry. Nitrogen transformations simulated include N fixation, mineralization and immobilization, volatilization, leaching, ammonification, nitrification, and denitrification. Losses in the form of nitrous oxide (N_2O) are controlled by mineral N availability, organic carbon content, water-filled pore space (in turn affected by climate and soil texture), and soil pH.

We post-processed our DayCent simulation results for this assessment as follows:

Harvest – Harvested herbaceous and woody biomass carbon amounts are reported via the ‘crmvst’ and ‘tcrem’ parameters of the DayCent list.100 output, respectively. These parameters are reported on an annual basis and were summed and translated to a daily time-step series within our analysis code. Our switchgrass simulations assumed harvest of 95% of total aboveground switchgrass biomass, with the remaining 5% left on the field as surface litter. Our secondary forest clear-cutting scenarios assumed harvest of all live stems and branches and burning of all remaining foliage and dead downed stems and branches.

Ecosystem carbon storage – The size of various above- and belowground carbon pools is reported in the dc_sip.csv model output on a daily time step. Note that DayCent models crop and grass growth with one set of carbon pools, and forest growth with another. Our analysis code calculated intermediate carbon pool sizes as well as total above- and belowground ecosystem carbon across both the both crop/grass and forest pools each day, as summarized in Table S3. DayCent output is in units of g C m^{-2} y^{-1}, which our code then converted to both a Mg C ha^{-1} y^{-1} basis and a Mg CO_2e ha^{-1} y^{-1} basis. Average annual NECB (and its above- and belowground constituents) over the first 30 years of simulation was evaluated in this manner for Figs. 1 and 4.

Net primary production & heterotrophic respiration – Simulated daily NPP is reported in the dc_sip.csv model output, which we then converted to a Mg C ha^{-1} y^{-1} basis. Daily heterotrophic respiration (R_h) was calculated by difference from DayCent-simulated NPP, NECB, and harvest results using eqn. [1] in the Methods section.

Nitrous oxide – Simulated daily N_2O emissions from soil nitrification and denitrification processes are reported individually in the DayCent nflux.out output in units of g N ha^{-2}. Our analysis code summed these two sources and converted the result to a Mg CO_2e ha^{-1} basis.

Simulated N_2O emissions were relatively small, and thus were combined with the bioenergy supply chain (BSC) emissions term to simplify the display of Fig. 4.

Figures S7–9 provide an illustrative example of simulated changes in above- and below-ground carbon storage after retirement of Iowa cropland and conversion to native forest types, grassland, or cultivation of current-day switchgrass, a disaggregation of the averaged results presented in Fig. 1. The definitions of the individual carbon pools shown are summarized in Table S3.

DayCent forest calibration

We created new regionally specific parameterizations to simulate native forest growth at the different case study sites based on the forest yield tables reported in Smith *et al.* 2006 (35), which are derived from US Forest Service inventory data and models. That reference includes forest yield tables describing changes in stand carbon density for both forest growth following clearcut harvest of prior existing forest (Smith *et al.* 2006, Appendix A) and for new forest growth on land previously under other land cover (Appendix B). Those two cases have the same carbon density values for live trees, standing dead trees, and understory vegetation, but the 'forest-following-forest' case includes high initial levels of down dead wood and forest floor litter, and the 'new-forest' case has lower initial soil carbon.

Our DayCent calibration consisted of an automated ensemble approach based on six combinations of SSURGO soil and NARR weather selected at random from the full range present within each case study county. We performed model spin-up for both 'forest-following-forest' and 'forest-following-crop' cases to align with the yield tables in Smith *et al*. 2006 Appendix A and B, respectively. We then simulated forest regrowth for each element of both ensembles, calculated total living and dead biomass C density on an annual time step (Table S4), and computed the average values across each ensemble. We ensured a conservative comparison for our bioenergy scenarios by calibrating DayCent's forest productivity potential and symbiotic nitrogen fixation to match total (live + dead) stand carbon density for the most productive forest type within each Smith *et al.* 2006 region from stand age 0–85 years, bringing the DayCent-simulated results as close as possible to—but not below—the target values.

Nitrogen inputs from atmospheric deposition and symbiotic nitrogen fixation are an important control on successional forest productivity, though afforestation/reforestation soil nitrogen dynamics are highly variable and difficult to generalize (87–89). Leaving atmospheric deposition inputs at their default values, we adjusted symbiotic nitrogen fixation for broad consistency with soil total nitrogen trend data from two representative afforestation studies (69, 70) and to minimize divergence between the forest-following-forest and forest-following-crop ensembles due to differing site fertility conditions (i.e., different initial soil organic matter levels). Finally, we adjusted tree tissue mortality so the forest-following-crop ensemble dead biomass carbon densities would best match the corresponding values in Smith *et al*. 2006 Appendix A. Note that forest floor (i.e., surface litter) and soil organic carbon were not included in the comparison, as DayCent models these quantities in a more explicit manner than does Smith *et al*. 2006. Final forest calibration results are detailed in Fig. S10.

Table S1. Detailed ecosystem & biorefinery modeling results (30-year simulation averages).

	Current biofuels	Future biofuels	Future biofuel + CCS	Grassland restoration	Reforestation
Ecosystem performance					
NPP (Mg C ha^{-1} y^{-1})	8.7 (7.0–11.7)	14.2 (11.3–19.0)		4.9 (3.4–6.9)	3.7 (1.8–5.0)
NECB (Mg C ha^{-1} y^{-1})	0.32 (0.11–0.60)	0.63 (0.33–1.06)		0.71 (0.54–1.00)	2.3 (1.0–3.4)
NECB:NPP ratio	0.04 (0.01–0.07)	0.05 (0.02–0.07)		0.15 (0.09–0.22)	0.61 (0.55–0.66)
Harvest (Mg C ha^{-1} y^{-1})	5.7 (5.0–6.7)	9.3 (8.2–11.0)		NA	
Harvest:NPP ratio	0.67 (0.57–0.72)	0.67 (0.58–0.73)			
Yield[a] (Mg dry biomass ha^{-1} y^{-1})	11.5 (10.2–13.5)	18.4 (16.2–21.8)			
Biorefinery performance					
Energy efficiency[b]	**43.3%**	**71.2%**	**67.6%**		
Ethanol	40.4%	54.1%	54.1%		
FT liquids	NA	15.8%	15.8%		
Electricity	3.0%	1.3%	-2.3%		
Fraction biomass C in fuel	**26.3%**	**46.1%**	**46.1%**		
Fraction biomass C emitted at biorefinery	**73.7%**	**52.2%**	**4.1%**		
Fraction biomass C sequestered via CCS or char	**0%**	**1.7%**	**49.8%**		
CCS + char sequestration rate (Mg C ha^{-1} y^{-1})	**NA**	0.13 (0.12–0.15)	4.8 (4.2–5.7)		
(CCS+char):NPP ratio	**NA**	0.009 (0.008–0.010)	0.34 (0.30–0.37)		

[a]based on the cellulosic biomass chemical composition specified in Laser *et al.* 2009 (40)
[b]energy content of biorefinery products as a fraction of input dry feedstock lower heating value

Table S2. LUC factors and calculations.

Feedstock	**Switchgrass**					**Miscanthus**			**Perennial grasses**
Model	FASOM -FAPRI	GTAP 1	GTAP 2	GTAP 3 CCLUB	GCAM	GTAP 1	GTAP 2	GTAP 3 CCLUB	GLO-BIOM
Reference	(76)	(78, 79)	(78, 80)	(45, 78)	(77)	(78, 79)	(78, 80)	(45, 78)	(81)
Reported total induced LUC (g CO_2e MJ^{-1})	13.4	2.7[a]	8.9[b]	0.5[b]	45	-10[a]	-7.9[b]	-17.1[b]	-8.1
Reported international LUC factor (g CO_2e MJ^{-1})	15.6[c]	6.7[d]	—	7.1[e]	-1.3[f]	1.7[d]	—	2.2[e]	—
Biofuel shock size (GL ethanol y^{-1})	30	27			34	27			—
Energy crop yield (Mg ha^{-1} y^{-1})	15.1	10.1			~20	17.5			11.5[g]
Total direct land use (Mha)	5.1	9.5			10	5.1			—
Adjusted total induced LUC factor (Mg CO_2e ha^{-1} y^{-1})	1.7	0.16	0.53	0.03	3.3	-1.1	-0.89	-1.9	-0.57
Adjusted international LUC factor (Mg CO_2e ha^{-1} y^{-1})	1.9	0.40	—	0.42	-0.09	0.19	—	-0.24	—

[a]base-case estimate considered in Dunn *et al.* 2013 (90)
[b]average across the range of results reported
[c]estimated from Pavlenko & Searle 2018 (44), Figure 4 (LUC effects only)
[d]estimated from Pavlenko & Searle 2018 (44), Figure 7
[e]estimated from Qin *et al.* 2016 (45), Figure 5
[f]estimated from Pavlenko & Searle 2018 (44), Figure 9
[g]average for switchgrass and Miscanthus, across three assessment regions and two time periods (current and future)

Table S3. DayCent variables for NECB calculation.

NECB component	Intermediate carbon pool	DayCent output	DayCent output pool description (all in units of g C m^{-2})
Total above-ground C (AGC)	Aboveground live crop/grass C (AGL crop)	aglivc	Above ground live carbon for crop/grass
	Aboveground dead crop/grass C (AGD crop)	stdedc	Standing dead carbon for crop/grass
	Aboveground live forest C (AGL tree)	rleavc	Leaf live carbon for forest
		fbrchc	Fine branch live carbon for forest
		rlwodc	Large wood live carbon for forest
	Aboveground dead forest C (AGL tree)	wood1c	Dead fine branch carbon
		wood2c	Dead large wood carbon
	Surface litter	strucc(1)	Carbon in structural component of surface litter
		metabc(1)	Carbon in metabolic component of surface litter
Total below-ground C (BGC)	Belowground live crop/grass C (BGL crop)	bglivcj	Juvenile fine root live carbon for crop/grass
		bglivcm	Mature fine root live carbon for crop/grass
	Belowground live forest C (BGL tree)	crootc	Coarse root live carbon for forest
		frootcj	Juvenile fine root live carbon for forest
		frootcm	Mature fine root live carbon for forest
	Soil litter	strucc(2)	Carbon in structural component of soil litter
		metabc(2)	Carbon in metabolic component of soil litter
		wood3c	Dead coarse root carbon
	Soil organic matter	som1c(1)	Carbon in surface active soil organic matter
		som1c(2)	Carbon in soil active soil organic matter
		som2c(1)	Carbon in surface slow soil organic matter
		som2c(2)	Carbon in soil slow soil organic matter
		som3c	Carbon in passive soil organic matter

Table S4. Variables considered in DayCent forest calibration.

Carbon pools for comparison	Smith 2006 Appendix A data sources	DayCent output name	DayCent pool description (all in units of g C m^{-2})
Total living biomass C	live trees + understory vegetation (includes stems, branches, foliage, coarse roots)	rlwodc	Large wood live carbon for forest
		fbrchc	Fine branch live carbon for forest
		rleavc	Leaf live carbon for forest
		crootc	Coarse root live carbon for forest
Total dead biomass C	standing dead trees + down dead wood (includes stems, branches, foliage, coarse roots, and surface fuels)	wood1c	Dead fine branch carbon
		wood2c	Dead large wood carbon
Excluded	forest floor, soil organic carbon	All other DayCent C pools	

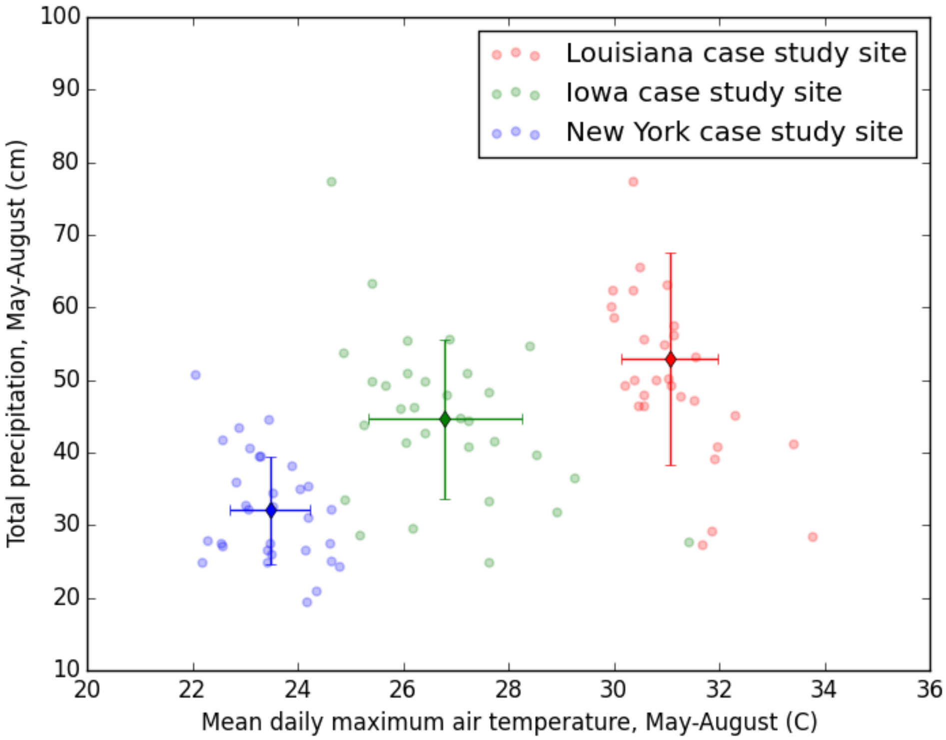

Fig. S1. Comparison of growing-season temperature and precipitation across the case study sites. Based on the North American Regional Reanalysis data (65). Points show records for individual years included in the 1979–2009 record. Diamonds indicate inter-annual means, with error bars showing one standard deviation.

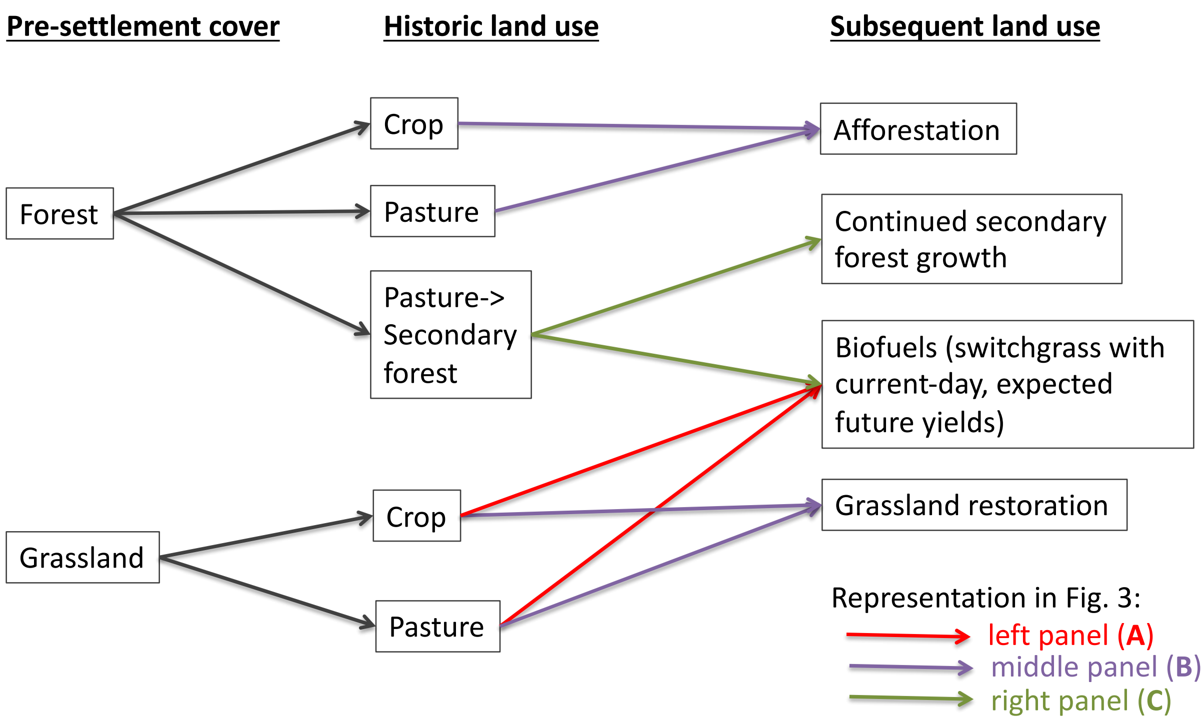

Fig. S2. DayCent simulation scenario matrix. Model initialization requires representation of pre-settlement land cover and historic land use. Arrow colors show which scenarios are included in which panel of Fig. 3, as indicated in the key.

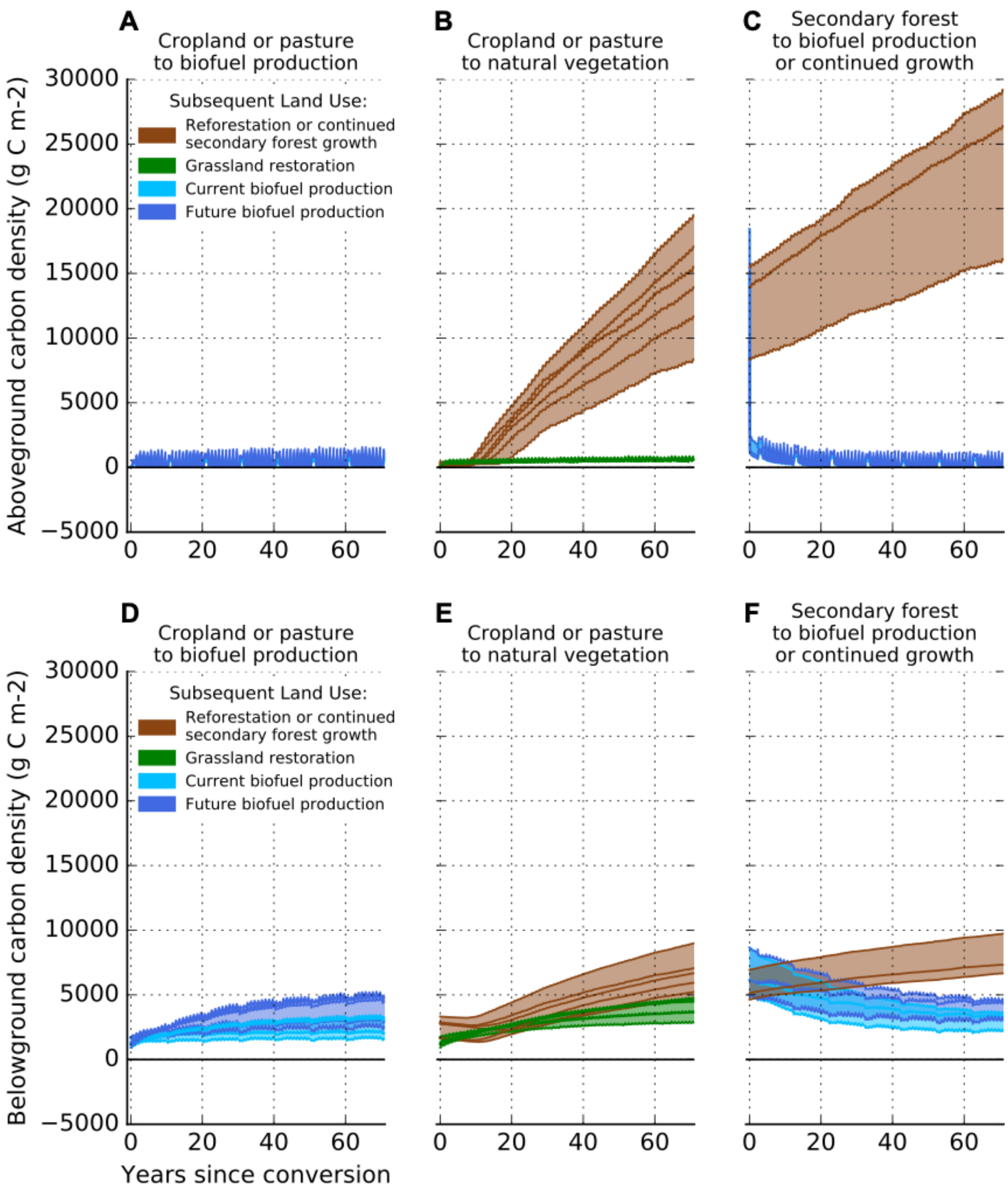

Fig. S3. Cumulative above- (A, B, C) and below-ground (D, E, F) NECB versus time. Results plotted individually for scenarios of (**A, D**) biofuel production on former agricultural land, (**B, E**) natural vegetation restoration on former agricultural land, and (**C, F**) secondary forest harvest and conversion to biofuel production versus continued undisturbed growth, evaluated at the three case study sites.

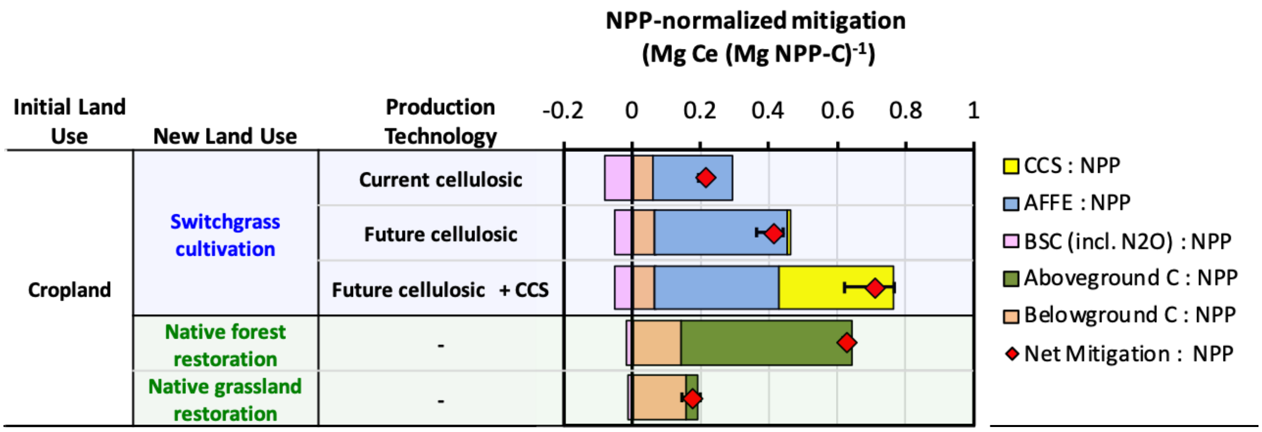

Fig. S4: NPP-normalized mitigation shares. Results for bioenergy and vegetation restoration scenarios on former cropland re-factored in units of metric tonnes of carbon equivalent (Mg Ce) mitigated per tonne of NPP carbon (Mg NPP-C) fixed. This illustrates the relative effectiveness of different scenarios at storing biogenic carbon and/or mitigating fossil energy emissions per unit of plant productivity, independent from the differences in plant productivity between scenarios.

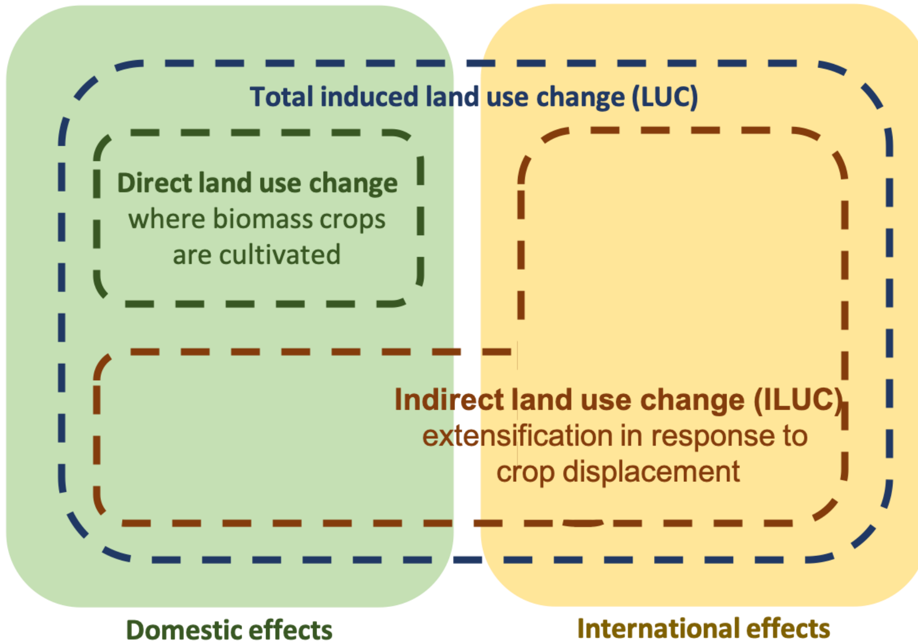

Fig. S5. Land use change emissions. This conceptual diagram illustrates the difference between direct land use change, the domestic and international components of indirect land use change (ILUC), and total induced LUC as the sum of all direct and indirect land use change effects combined.

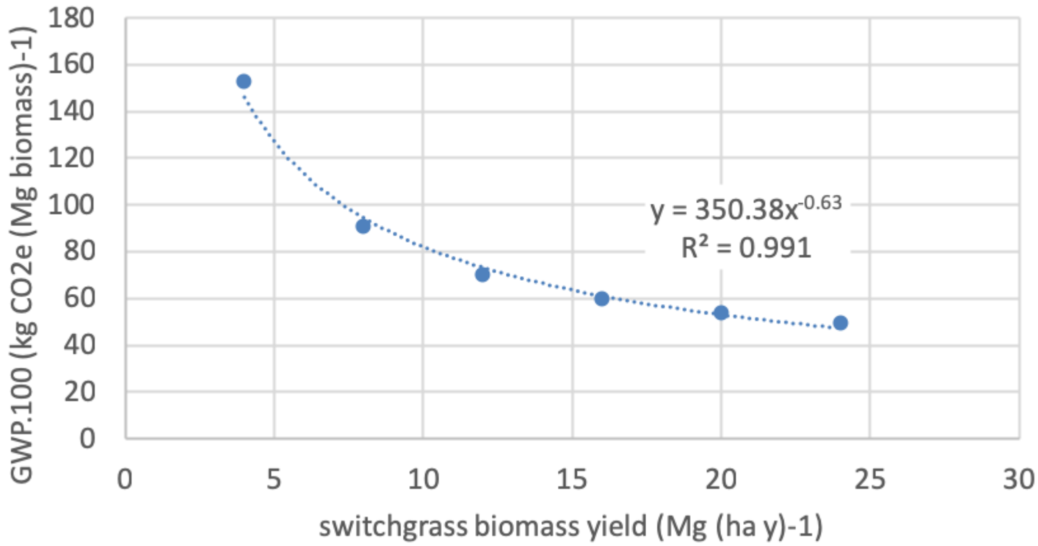

Fig. S6: Farm-to-biorefinery-gate GHG footprint of switchgrass biomass as a function of yield. Includes farm inputs and energy use, biomass harvest, and farm–biorefinery transport. Excludes changes in soil carbon and soil nitrous oxide emissions.

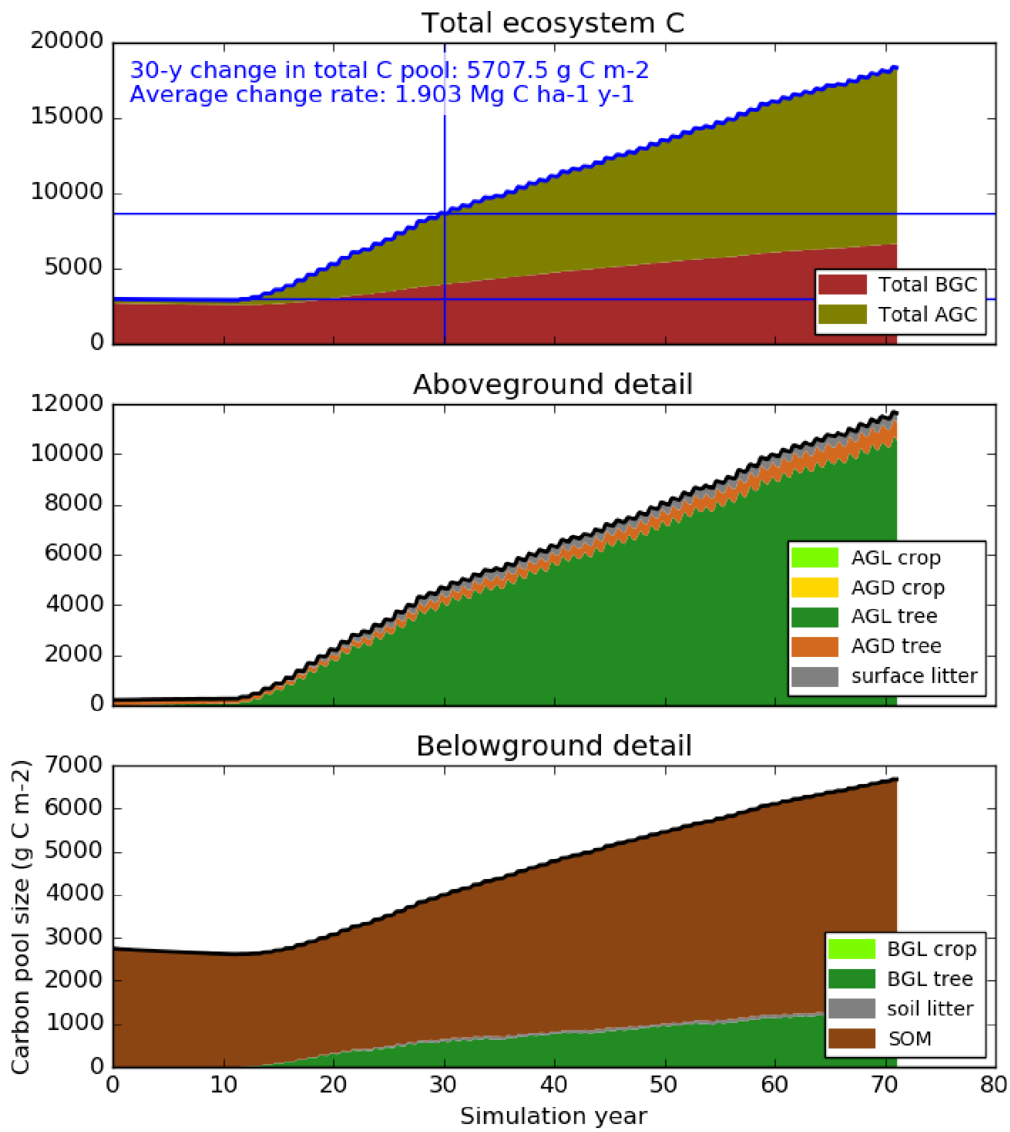

Fig. S7: DayCent simulation detail for reforestation on former Iowa cropland. Change in NECB over time (top panel) and associated above- and belowground carbon pool detail (middle and lower panel, respectively), with pools defined as per Table S3. Calculation of the 30-year average annual NECB is illustrated with blue lines. In this scenario, most of the increase in ecosystem carbon storage is due to aboveground live biomass (specifically tree stems, branches, and foliage).

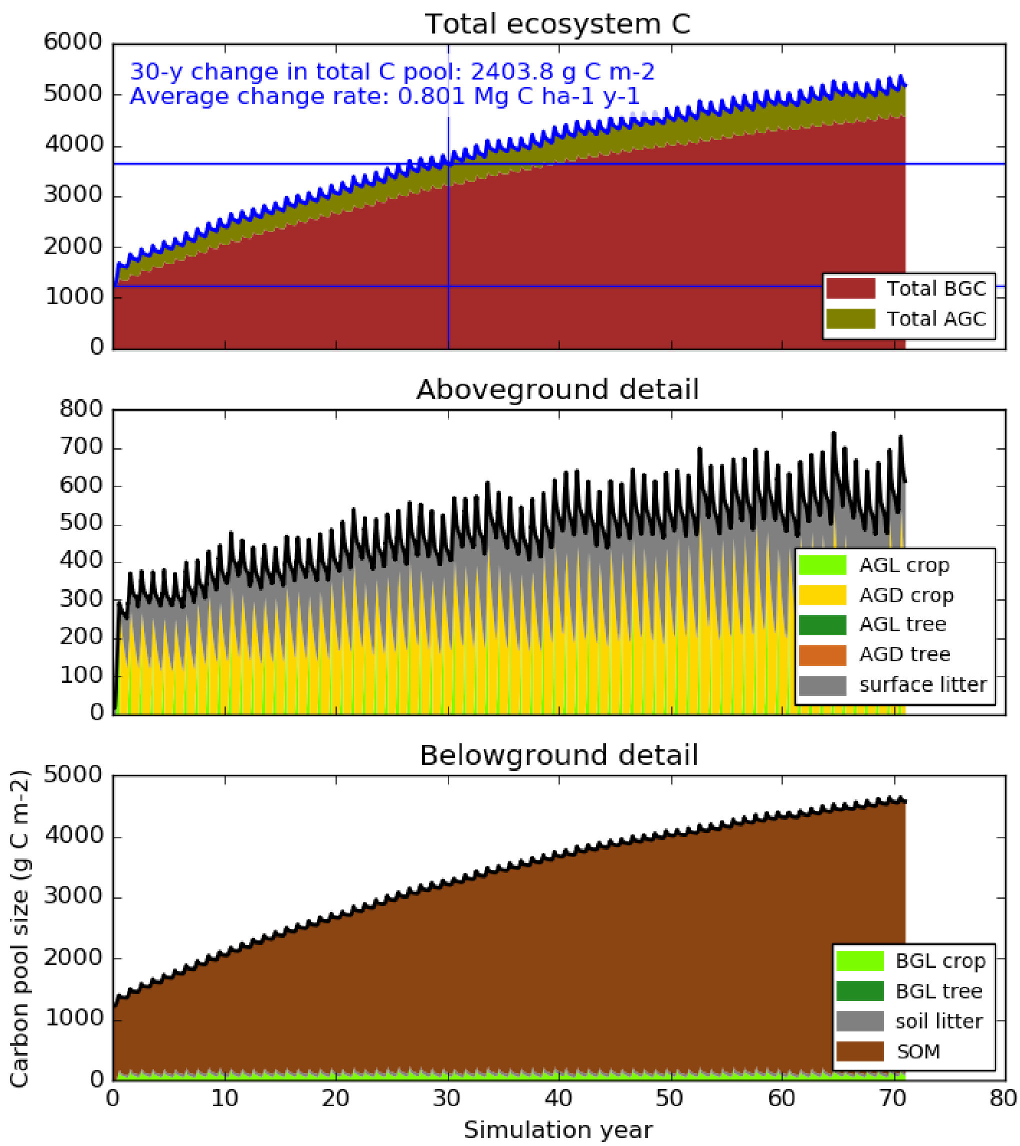

Fig. S8: DayCent simulation detail for grassland restoration on former Iowa cropland. Note the changes in y-axis scaling from the previous figure. Compared to the previous reforestation scenario, soil organic matter carbon increases by a similar amount over the course of the grassland restoration simulation, but aboveground carbon storage remains modest, dominated by standing dead biomass and surface litter (yellow and grey colors in the middle panel). The saw-tooth pattern in total aboveground carbon is driven by the grass growing season between spring green-up and fall senescence.

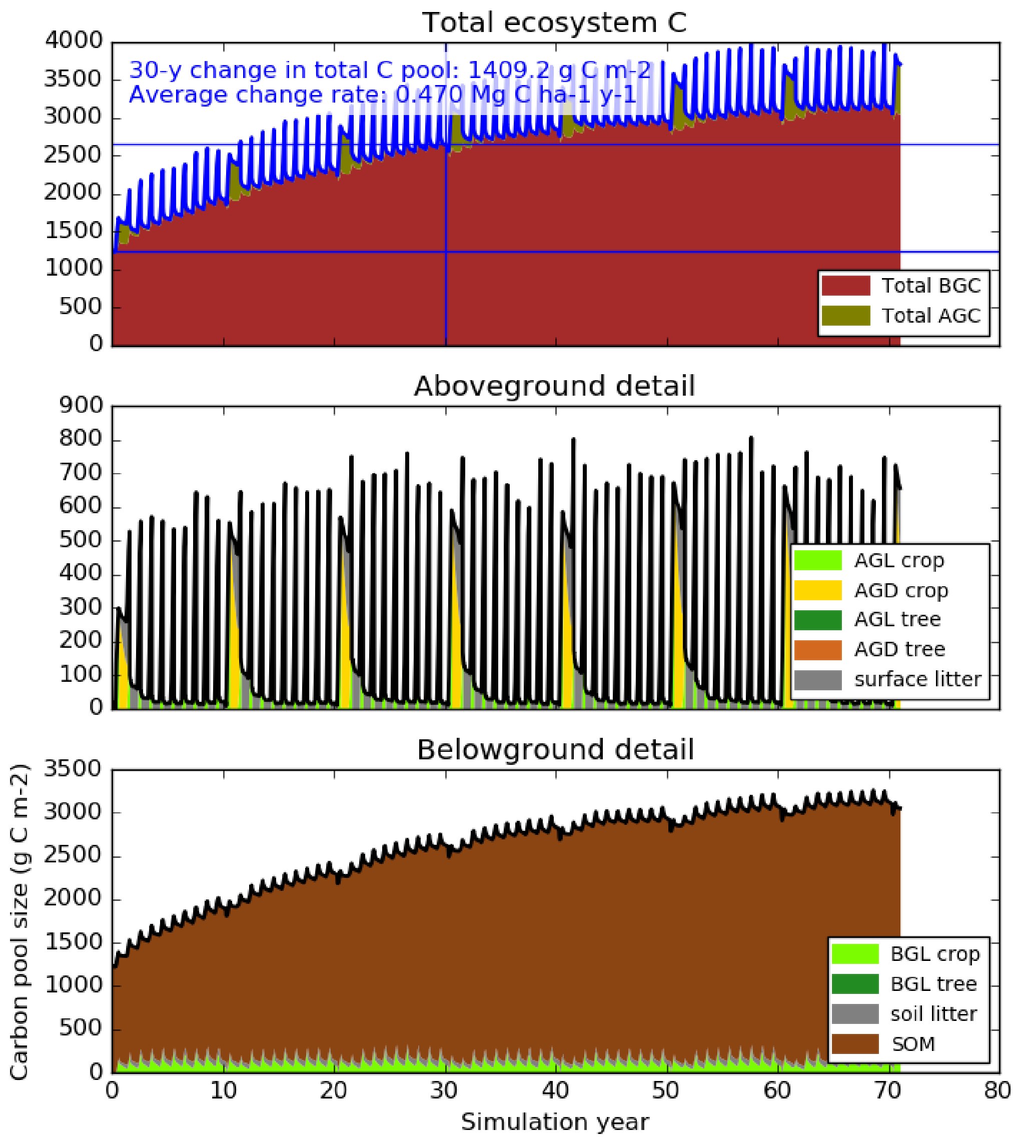

Fig. S9: DayCent simulation detail for current-day switchgrass production on former Iowa cropland. Note the changes in y-axis scaling from the previous figure. The fluctuation in aboveground dead crop biomass every 10 years is due to stand replanting (switchgrass not harvested the year of planting). Compared to the previous grassland restoration scenario, soil carbon increase is more modest due to removal of aboveground biomass during harvest and the subsequent lack of surface litter as a soil organic matter input. However, simulated productivity is much higher due to management (fertilizer application that relieves nitrogen limitations on growth) and lack of self-shading from accumulated standing dead biomass.

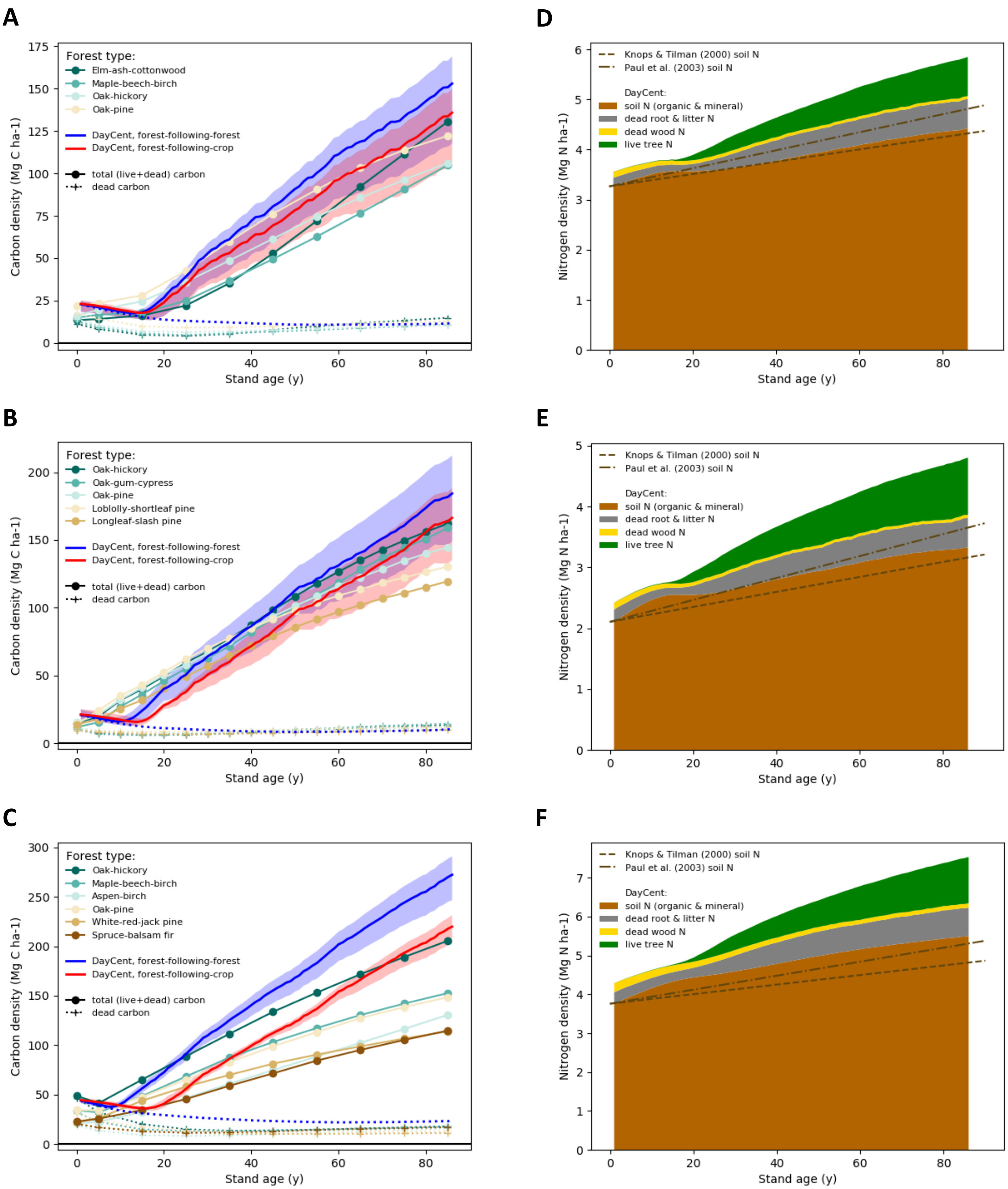

Fig. S10. DayCent forest calibration results. Showing stand carbon and nitrogen density results, respectively, for the Iowa (A and D), Louisiana (B and E), and New York (C and F) case study sites, as compared to calibration targets. For the carbon plots A–C, different forest types are show in different shades of blue to brown, with dead carbon shown with plus-sign markers and dotted lines, and total stand carbon shown with circular markers and solid lines. Corresponding DayCent simulation results are shown in red (forest-following-crop) and blue (forest-following-forest).